9-1-2020

Shared Neural Substrates of Perception and Memory: Testing the Assumptions and Predictions of the Representational-Hierarchical Account

D. Merika W. Sanders
University of Massachusetts Amherst

SHARED NEURAL SUBSTRATES OF PERCEPTION AND MEMORY: TESTING THE ASSUMPTIONS AND PREDICTIONS OF THE REPRESENTATIONAL-HIERARCHICAL ACCOUNT

A Dissertation Presented

by

D. MERIKA W. SANDERS

Submitted to the Graduate School of the
University of Massachusetts Amherst in partial fulfillment
of the requirements for the degree of

DOCTOR OF PHILOSOPHY

September 2020

Psychology

SHARED NEURAL SUBSTRATES OF PERCEPTION AND MEMORY: TESTING THE ASSUMPTIONS AND PREDICTIONS OF THE REPRESENTATIONAL-HIERARCHICAL ACCOUNT

A Dissertation Presented

by

D. MERIKA W. SANDERS

Approved as to style and content by:

_____
Rosemary Cowell, Chair

_____
Jeffrey Starns, Member

_____
Rebecca Spencer, Member

_____
Ethan Meyers, Member

_____
Caren Rotello, Department Head
Psychological and Brain Sciences

DEDICATION

From application

to dissertation, always

my cheerleader, Aus

ACKNOWLEDGMENTS

First, thank you to my advisor, Rosie Cowell, whose mentorship was instrumental to my academic success. Undoubtedly the generous commitment on her behalf, not limited to one-on-one tutorials on fMRI analysis during my first year, was critical in establishing the research skill set I utilized here. Moreover, her unwavering support and genuine interest in my ideas has nurtured my confidence as an independent scientist.

Second, I would like to thank the members of my dissertation committee: Jeff Starns, Bekki Spencer, and Ethan Meyers. The expertise they provided via thoughtful questions and feedback improved the research presented here. I would also like to thank the faculty members of the Cognition and Cognitive Neuroscience division that assisted me throughout my graduate career. This includes the members of my comprehensive exam committee (Dave Huber & Jeff Starns), my masters committee (Bekki Spencer & Jeff Starns), and my graduate statistics professor (Andrew Cohen). The guidance I received during each of these milestones was significant in bringing this work to fruition.

Third, I am grateful for my fellow students, both undergraduate and graduate. The efforts of research assistants in the Computational Memory and Perception Lab made stimulus creation and piloting possible. Further, the advice, expertise, and friendship provided by my graduate colleagues provided refuge on many hard, stressful days.

Finally, I would like to express my deepest gratitude to my family. So much of who and where I am today is due to their encouragement and unbelievable understanding when I had to prioritize my research. Especially to my little family: my husband, Austin, and our “dogaughter”, Annie. I could not have achieved this without your boundless love.

ABSTRACT

SHARED NEURAL SUBSTRATES OF PERCEPTION AND MEMORY: TESTING THE ASSUMPTIONS AND PREDICTIONS OF THE REPRESENTATIONAL-HIERARCHICAL ACCOUNT

SEPTEMBER 2020

D. MERIKA W. SANDERS, B.S., ST. LAWRENCE UNIVERSITY

M.S., UNIVERSITY OF MASSACHUSETTS AMHERST

Ph.D., UNIVERSITY OF MASSACHUSETTS AMHERST

Directed by: Rosemary A. Cowell

Proponents of the representational-hierarchical (R-H) account claim that memory and perception rely on shared neural representations. In the ventral visual stream, posterior brain areas are assumed to represent simple information (e.g. low-level image properties), but the complexity of representations increases toward more anterior areas, such as inferior temporal cortex (e.g., object-parts, objects), extending into the medial temporal lobe (MTL; e.g. scenes). This view predicts that brain structures along this continuum serve both memory and perception; a structure's engagement is determined by the representational demands of a task, rather than the cognitive process putatively involved.

In a neuroimaging study, I searched for the transition from feature-based representations to conjunction-based representations along this pathway. In the first scan session, participants viewed two stimulus sets with different levels of complexity: fribbles (novel 3D objects) and scenes (novel, computer-generated rooms). According to the R-H account, a neural feature-code for both fribbles and scenes should reside in

posterior ventral visual stream. I predicted a transition to conjunction-coding toward MTL, with the transition for the simpler stimulus set (fribbles) occurring earlier.

Next, I measured memory signals while varying (1) stimulus complexity and (2) type of retrieved information (features or conjunctions). In a second scan session, participants completed a recognition memory task for fribbles and scenes, with three mnemonic classes of item. Novel items comprised novel features combined in a novel conjunction; Recombination items possessed features that had been seen in the first session, but never within the same item (i.e., familiar features, but novel conjunctions); and Familiar items comprised familiar features and familiar conjunctions. Under the R-H account, a memory task that requires only the retrieval of feature-based information should recruit visual cortex rather than MTL. Further, these "feature memory" signals should map onto feature-coding regions found in the first session.

Analyses revealed that visual regions, outside of MTL, contained (1) more information about individual features than conjunctions of features (first session data), and (2) the greatest signal for feature memory (second session data). Thus, cortical regions that best represented feature information during perception also best signaled feature information in memory and were located outside MTL.

TABLE OF CONTENTS

Page

ACKNOWLEDGMENTS v

ABSTRACT vi

LIST OF TABLES x

LIST OF FIGURES xi

CHAPTER

1. INTRODUCTION 1

1.1 Overview 1
1.2 MTL Engagement during Perception 4
1.3 Content-dependent Engagement of MTL during Memory Retrieval 6
1.4 Ventral Visual Stream Engagement during Memory 10
1.5 Representational-Hierarchical Theory 14

1.5.1. Evidence for a Representational Hierarchy 19
1.5.2. Evidence for the Importance of Task Representational Demands 24

1.6 Aims 28

2. EXPERIMENT 31

2.1 Overview and Predictions 31
2.2 Method 34

2.2.1 Participants 34
2.2.2 Materials 34
2.2.3 Task 36
2.2.4 Experimental Design 37
2.2.5 Image Acquisition 39
2.2.6 fMRI Data Analyses 40

2.2.6.1 fMRI Data Preprocessing 40
2.2.6.2 Definition of Regions of Interest 40
2.2.6.3 ROI-Based Analyses of Feature-Conjunction Index 42
2.2.6.4 ROI-Based Analyses of Memory Scores 43
2.2.6.5 Searchlight Analysis of the Intersection of Representational Content and Memory Signals 46

2.3 Results 47

2.3.1 Behavioral Analysis 47
2.3.2 ROI-Based Analyses of Feature-Conjunction Index 48
2.3.3 ROI-Based Analyses of Memory Scores 51
2.3.4 Searchlight Analysis of the Intersection of Representational Content and Memory Signals 53

3. DISCUSSION 56

APPENDICES

A. IMAGING DATA PREPROCESSING 82

B. STIMULUS-SPECIFIC FEATURE-CONJUNCTION INDEXES 86

C. STIMULUS-SPECIFIC MEMORY SCORES 87

REFERENCES 88

LIST OF TABLES

Table Page

1. Extreme Outliers Omitted from Statistical Analyses....66

2. Discriminability of Mnemonic Stimulus Classes for Fribbles and Scenes....67

3. Ten Most Positive and Negative Voxels within Fribble FCI-ROIs....68

4. Ten Most Positive and Negative Voxels within Scene FCI-ROIs....69

LIST OF FIGURES

Figure Page

1. Illustration of Representational Organization 70
2. Simple Object Stimuli from Cowell et al. (2017), adapted with permission 71
3. Fribble Stimulus Set Examples 72
4. Scene Stimulus Set Examples 73
5. Scene Stimulus Set Recombination Examples 74
6. Experimental Design 75
7. Study Phase Classifier Accuracies by Stimulus Set and ROI Selection 76
8. Study Phase Feature-Conjunction Indexes (FCIs) by ROI Selection 77
9. Test Phase Memory Scores by ROI Selection 78
10. Study Phase Feature-Conjunction Indexes (FCIs) by Stimulus Set for Individual MTL ROIs Only 79
11. FCI-ROIs Defined via Searchlight Analysis of Study Phase Data 80
12. Test Phase Memory Scores for FCI-defined ROIs 81

CHAPTER 1

INTRODUCTION

1.1 Overview

Scientists have frequently adopted analogies to help describe complex problems in cognitive psychology and cognitive neuroscience. In order to convey the multitude of specific functional components of the mind, Cosmides & Tooby (1994) likened it to a Swiss army knife. Similar to how the bottle opener of a Swiss army knife serves a specific purpose distinct from that of the corkscrew, they proposed that each aspect of cognition involved distinct mechanisms and operated independently from any other aspect of cognition. This meant that visual perception, the instantaneous processing of the visual environment, is mechanistically and functionally separate from memory, the process of retaining that same information over a delay and later retrieving it.

Case studies demonstrating double-dissociations and the development of functional neuroimaging extended the Swiss army knife analogy beyond the mind to the brain (Kanwisher, 2006). Building on earlier animal findings (Blake, Jarvis, & Mishkin, 1977; Cowey & Gross, 1970; Gross, Cowey, & Manning, 1971; Iwai & Mishkin, 1968; Wilson, Kaufman, Zieler, & Lieb, 1972), imaging researchers continued to designate brain regions as “memory” or “perception” areas and assumed that those regions were selectively involved in their namesake tasks (e.g. the fusiform face area and the perception of faces; Kanwisher, McDermott, & Chun, 1997). Despite the simplistic nature of the Swiss army knife analogy, its modular framework claiming that brain regions are specialized for singular cognitive processes has had considerable influence in behavioral and neuroimaging research.

The influence of modular research is notably illustrated by the effect of the seminal work with patient H.M. on theories of long-term declarative memory (Rosenbaum, Gilboa, & Moscovitch, 2014; Squire, 2009). Contrary to the then held belief that memory is distributed across the cortex and integrated with perception (Lashley, 1950), studies on H.M. asserted that medial temporal lobe (MTL) structures, including hippocampus (HC), parahippocampal (PHC), entorhinal (ERC) and perirhinal (PRC) cortices, are uniquely critical for encoding, storing, and retrieving memory for events and facts (Scoville & Milner, 1957). Further, the combination of impaired memory and preserved perception following MTL lesions supported the notion that memory and perception were separable cognitive processes carried out by distinct brain regions. These findings served as the foundation for the MTL memory system account, in which MTL is important in establishing long-term memories, but is uninvolved in visual perception (Squire & Zola-Morgan, 1991).

The modular approach of the MTL memory system account continues to exert an influence on the field of memory research (e.g. Inhoff et al., 2019; S. Kim, Dede, Hopkins, & Squire, 2015; S.-H. Lee, Kravitz, & Baker, 2019; Suzuki, 2010). Under some theories extending this modular framework, long-term declarative memory has been further subdivided into separate sub-processes (i.e., recollection and familiarity) that are attributed to distinct MTL structures (e.g. Brown & Aggleton, 2001; Yonelinas, Aly, Wang, & Koen, 2010). Many experimental paradigms used in long-term memory retrieval research today (e.g. remember/know tests; item, source, and associative recognition tests) are explicitly designed to test either familiarity or recollection, or to tease apart these two mnemonic retrieval sub-processes. Additionally, many

neuroimaging or case study investigations of long-term declarative memory do not look beyond MTL (Davachi, 2006; Diana, Yonelinas, & Ranganath, 2007; Eichenbaum, Yonelinas, & Ranganath, 2007).

More recent theories of long-term declarative memory have evolved to include extra-MTL brain structures, such as prefrontal cortex or parietal cortex, in memory 'networks' (e.g. H. Kim, 2010; Ranganath & Ritchey, 2012; Rugg & Vilberg, 2013; Shimamura, 2011; Thakral, Wang, & Rugg, 2017). However, these memory networks reflect an evolution, rather than a rejection, of the modular approach to memory research. That is, researchers apply 'memory' functional labels to a *collection of nonadjacent brain areas* instead of *contiguous brain areas*, but the underlying approach of mapping component processes onto anatomical areas is the same. Therefore, although current memory research may not actively attempt to segregate memory and perception as modular research once did, much of it still operates within, and thus perpetuates, a Swiss army knife framework where memory and perception are separate component processes assumed to have distinct neural substrates.

Importantly, this modern modular framework critically fails to account for three categories of findings, some now well-documented and some newly emerging. These findings are that (1) engagement of MTL structures also occurs during perceptual tasks; (2) engagement of MTL structures during mnemonic tasks is content-dependent (i.e., varies by what information is to be remembered); and (3) engagement of brain areas along the ventral visual stream (regions traditionally thought of as visuo-perceptual areas) occurs during mnemonic tasks for simple, visual information. I review these three classes of findings next.

1.2 MTL Engagement during Perception

Despite the fact that patient H.M. had no apparent perceptual deficits, and PRC is included in the MTL memory system dedicated solely to memory, PRC is needed for some perceptual tasks, under specific circumstances. In a concurrent object discrimination task, two objects are presented simultaneously and, over several training trials in which responses to only one of the two objects is rewarded, participants learn to distinguish between rewarded objects and unrewarded objects. Early animal research indicated that PRC is involved in this task when "feature ambiguity" is present (Bartko, Winters, Cowell, Saksida, & Bussey, 2007b, 2007a; Bussey & Saksida, 2002; Bussey, Saksida, & Murray, 2002, 2003; Saksida, Bussey, Buckmaster, & Murray, 2006). Feature ambiguity occurs when individual features are shared between stimuli with different associated reward outcomes. For instance, a participant's response is rewarded when the features are a part of one object, but is not rewarded when the features appear as part of a different object. That is, the unique conjunction of features, rather than the individual features themselves, are key for discrimination. Animals with PRC lesions were unimpaired when feature ambiguity was at a minimum (i.e., features appeared only as part of rewarded *or* unrewarded objects), but were severely impaired compared to controls when feature ambiguity was at a maximum (i.e., all features appeared as part of both rewarded and unrewarded objects).

The finding that PRC is required to resolve feature ambiguity during concurrent object discrimination tasks was extended to humans by Barense et al. (2005). PRC-lesioned patients were increasingly impaired at discriminating between rewarded and unrewarded object stimuli when the number of features that appeared as part of both

rewarded and unrewarded objects (i.e., feature ambiguity) increased. However, patients with lesions to HC, but intact PRC, performed similarly to healthy controls, regardless of the level of feature ambiguity.

Subtle perceptual impairments following damage to the PRC extend beyond concurrent discrimination tasks to perceptual oddity tasks. In a perceptual oddity task, sets of objects are again presented simultaneously, so there is no need to remember the objects over any type of delay. The objective of this task is to determine which object of the set is different from all the others (i.e., the "odd object out") and the task is made more or less difficult by changing how similar the distracters within the set are from each other. For example, the task is easier when all distracters are the same object pictured from the same angle than when all distracters are the same object, but pictured from different angles. Both PRC-lesioned animals and humans performed similarly to non-lesioned controls during a perceptual oddity task when the "odd stimulus" could be discriminated from the distracters in the array by a simple feature, like color, shape or size (Bartko et al., 2007b, 2007a; Buckley, Booth, Rolls, & Gaffan, 2001; A. C. H. Lee, Buckley, et al., 2005). However, when the oddity task required discrimination based on complex representations of whole objects (e.g. when the distracters were the same face from different viewpoints, requiring a holistic representation to identify them as the same), those with PRC-lesions demonstrated significant deficits. Similar impairments were not found in participants with damage to HC, but intact PRC.

Although the above findings imply that HC is not required during perception of objects, there is additional evidence that HC is involved in perception for other classes of stimulus, for example scene stimuli (Barense, Henson, Lee, & Graham, 2010; A. C. H.

Lee, Barense, & Graham, 2005; A. C. H. Lee, Buckley, et al., 2005; A. C. H. Lee, Yeung, & Barense, 2012). For instance, individuals diagnosed with Alzheimer's disease, which predominantly causes atrophy in HC while affecting PRC to a lesser extent, or later in the disease progression, made more errors during a perceptual oddity task with scene stimuli than during the analogous task performed with faces (A. C. H. Lee, 2006). Additionally, HC-lesion patients made an increasing number of errors in a concurrent discrimination task as the level of feature ambiguity of scene stimuli increased (A. C. H. Lee, Bussey, et al., 2005).

There is also a large body of evidence, stretching back decades, that the role of HC includes general spatial cognition (e.g. O'Keefe & Dostrovsky, 1971; O'Keefe & Nadel, 1978), as well as (discovered more recently) scene construction (e.g. Hassabis, Kumaran, Vann, & Maguire, 2007), and episodic future thinking involving scenes (e.g. Palombo, Hayes, Peterson, Keane, & Verfaellie, 2016). Owing to the functional diversity ascribed to HC on the basis of these results, the region may be better characterized as a critical region for general spatial context processing, which is called upon for a wide range of cognitive functions, including memory and perception (Maguire, Intraub, & Mullally, 2015; Mullally & Maguire, 2013; Zeidman, Mullally, & Maguire, 2015). However, an extension of the role of HC, or any other MTL structure, beyond a singular mnemonic function is incompatible with a traditional modular framework in which brain regions, or specific brain networks, are uniquely engaged in one cognitive function that operates independently from any other aspect of cognition.

1.3 Content-dependent Engagement of MTL during Memory Retrieval

Many dominant theories of long-term declarative memory retrieval characterize it as two distinct mnemonic retrieval processes that are modulated by different MTL areas. Familiarity-based memory is associated with the event of "knowing" that an item has been seen previously without the ability to remember the contextual details of the episode, whereas recollection is associated with the event of "remembering" the episode's contextual details, including the spatial and temporal context (Mandler, 1980). Early process-based accounts explicitly linked familiarity and recollection to medial temporal neocortex and HC, respectively (Aggleton & Brown, 1999; Norman & O'Reilly, 2003), but more recently the Binding of Items and Context (BIC) model additionally assumes that medial temporal neocortical structures differ in terms of the type of stimulus representations they process (Diana, Yonelinas, & Ranganath, 2007; Eichenbaum, Yonelinas, & Ranganath, 2007).

According to the BIC model, PRC processes information pertaining to item representations, while PHC processes information pertaining to contextual, especially (but not limited to) spatial, representations. Item representations within PRC best support familiarity because familiarity judgements are based on item recognition alone and do not require the retrieval of contextual details. In contrast, PHC contributes to recollection, which requires the retrieval of the specific contextual details of an event, because it contains representations of contexts. HC is essential for recollection because it is theorized to bind PRC item representations and PHC context representations into item-context associative representations, and so it is needed for the key process of recollection in which one aspect of a memory (e.g., an item) cues retrieval of another associated aspect (e.g., the encoding context).

Evidence for the claims of the BIC model appears to be substantial. Many studies support the role of PRC in item recognition (e.g. Eacott et al., 1994; Meunier et al., 1993; Winters, Forwood, Cowell, Saksida, & Bussey, 2004), and cued recall fMRI studies support the role of HC in recollection (e.g. Davachi, Mitchell, & Wagner, 2003; Diana et al., 2007; Hannula, Libby, Yonelinas, & Ranganath, 2013; Staresina, Cooper, & Henson, 2013). In these cued recall studies, participants often study paired associates, for example, pictures of objects paired with pictures of scenes. At test, participants are cued with either the scene and asked to recall the object (i.e., item retrieval) or the object and asked to recall the scene (i.e., context retrieval). Researchers found that PHC was activated for successful context retrieval, and PRC was activated for successful item retrieval (Staresina et al., 2013). In contrast, HC was activated for retrieval of both item and context, and to a similar extent. Staresina et al. (2013) also used dynamic causal modeling to explore the flow of information between MTL regions. When objects cued retrieval of scenes, information flowed from PRC to PHC, but when scenes cued retrieval of objects, information flowed from PHC to PRC. Additionally, regardless of what stimulus type served as the cue or the target, HC further facilitated the flow of information between cue and target brain areas.

However, traditional tests of recollection and familiarity have conflated differences in content with differences in mnemonic retrieval processes. That is, familiarity has consistently been tested using singly presented items (i.e., a non-associative task), whereas recollection has consistently been tested using associative pairs. The above findings could instead reflect differences in the *information* processed within a MTL structure, rather than differences in retrieval processes/operations that each

MTL structure can compute (Cowell, Bussey, & Saksida, 2010; Ross, Sadil, Wilson, & Cowell, 2018). According to an alternative account (the Representational-Hierarchical account detailed below), PRC is engaged whenever processing involves objects; PHC is engaged for processing of more complex spatial information; and HC is engaged whenever the task requires processing the complex conjunction (or association) between items and context (often involving spatial properties). Consequently, recollection and familiarity can occur in any MTL structure, depending on whether the representations housed in that MTL structure are required for the task of recollecting or for judging familiarity, which in turn depends on *what information* is being recollected or judged.

In an attempt to tease apart process and representation based accounts, Ross et al. (2018) created a cued recall paradigm with non-associative stimuli. While in a scanner, participants viewed images of objects and scenes. At test, participants were cued with circular patches taken from studied and unstudied images and asked if they specifically remembered the original whole image. For object stimuli, using a part of the image as the cue avoided HC associative representations that are usually involved during cued recall tasks. Instead, only intra-item, pre-experimentally established associations between object parts were required for successful completion of the task.

The results indicated that HC engagement was dependent on the content of the to-be-retrieved memory during the recall task: HC was engaged during scene recall, but not during object recall; in contrast, PRC was engaged during both object and scene recall[1]. Further, unlike Staresina et al. (2013), in which recall involved retrieval of associative memories, Ross et al. (2018) did not find evidence for feedback from HC to other regions

[1] Ross et al. (2018) note that PRC may have been engaged during scene recall because scenes and scene parts frequently contain objects.

during part-cued object or scene recall. Instead, information flow during object recall was driven by lateral occipital cortex (LOC) and information flow during scene recall was driven by PHC. Ross et al. (2018) concluded that MTL engagement during memory retrieval is content-dependent rather than process-dependent. This claim finds additional support in a unique case study, described next.

Lacot et al. (2017) reported a case study in which patient JMG had extensive MTL damage that spared only the right HC in its entirety, meaning PRC was damaged bilaterally. On a variety of memory tasks JMG demonstrated impaired performance when to-be-remembered items were objects, regardless of whether the task was intended to test familiarity or recollection. However, when the object stimuli were replaced with scene stimuli, JMG performed similarly to control subjects. Thus, there is both neuroimaging (Ross et al., 2018) and case study (Lacot et al., 2017) evidence that engagement of MTL structures during a memory task varies depending on what type of information is to be remembered. Further, this evidence is in direct opposition to a Swiss army knife modular approach, in which memory is said to be organized according to component processes.

1.4 Ventral Visual Stream Engagement during Memory

There is a growing body of neuroimaging evidence that brain regions along the ventral visual stream – that is, regions previously thought to be engaged exclusively in sensory and perceptual processing – are engaged during long-term memory retrieval tasks if the to-be-remembered information is purely visual and sufficiently low-dimensional. It has been known for some time that LOC preferentially processes shape and object information during visual perception (Grill-Spector, 2003; Grill-Spector, Kourtzi, &

Kanwisher, 2001; Grill-Spector et al., 1999; Malach et al., 1995; Ungerleider & Mishkin, 1982). Karanian & Slotnick (2015) investigated the location of memory signals for this level of 'simple' visual information by presenting intact shapes and scrambled shapes in unique colors to participants while being scanned. Participants were later cued with the unique colors, asking them to retrieve whether the corresponding shape had appeared as "intact" or "scrambled" during the encoding phase. Neural activity associated with successful retrieval of shape memory was found in LOC, the same region involved in perceptual processing of shape information. Further, false memories for shape (i.e., incorrectly recalling a scrambled shape as intact) also elicited neural activity in LOC, but to a lesser extent than true memories for shape (Karanian & Slotnick, 2017).

Another region in the ventral visual stream, V8, which lies posterior to LOC and is known to have a role in color processing, has also been shown to be involved in memory for color. During an encoding scan, participants viewed a series of colored and gray abstract shapes (Slotnick, 2009). After a delay and while participants were still in the scanner, researchers then presented another series of abstract shapes, some of which had been seen during the encoding scan and others that had not. Participants were asked to correctly classify each shape into one or three categories: seen during encoding in color ('old-colored'), seen during encoding in gray ('old-gray'), or not seen at all ('new'). Area V8, which is color-selective during retinotopic mapping (Hadjikhani, Liu, Dale, Cavanagh, & Tootell, 1998), exhibited significantly greater activation on trials associated with accurate color item and context memory (i.e., correct 'old-colored' response) than for trials with accurate color item but inaccurate color context memory (i.e., incorrect 'old-gray' response during an old-colored trial) or trials with accurate gray item and

context memory (i.e., correct ‘old-gray’ response). Thus, V8, an area that selectively processes color information during perceptual tasks, also demonstrated activity associated with successful memory retrieval of color-specific information.

Feature-specific memory signals within ventral visual stream have even been found as early as primary visual cortex, V1. This was recently explored in a study with mice (Cooke, Komorowski, Kaplan, Gavornik, Jeffrey, & Bear, 2015). Researchers observed that head-fixed mice move their paws when presented with visual stimuli and this visually-induced fidget (or “vidget”) could be measured with a piezo-electric sensor. In a similar manner to visually evoked potentials in V1, the intensity of vidgets was found to vary systematically when manipulating the contrast and spatial frequencies of sinusoidal grating stimuli. Additionally, pharmacological blocking of neural activity in V1 resulted in diminished vidgets. Thus, vidgets appear to require the engagement of V1 and can be used to measure processing of feature-specific information for sinusoidal grating stimuli. When grating stimuli with a particular orientation were repeatedly presented over several days, the intensity of vidgets diminished, reflecting orientation-selective habituation as the stimulus orientation became familiar. Additionally, following habituation, presentation of stimuli with a novel orientation elicited significantly more intense vidgets than for stimuli with the familiar orientation. However, the difference in vidget magnitude between familiar and novel orientations was eliminated when synaptic plasticity was restricted in V1. These findings suggest that engagement of V1 is critical for recognition memory of orientation information.

Memory signals in early visual cortex have also been found in studies with humans. Thakral, Slotnick, & Schacter (2013) presented abstract colored shapes to

participants while they were being scanned; critically, the abstract shapes were presented to the left or right of a central fixation point. During a mnemonic recognition test, items were presented centrally and participants classified each item as 'old-left', 'old-right', or 'new'. Accurate item and spatial context memory (i.e., correct 'old-left' or 'old-right' responses) engaged primary visual regions V1 (Brodmann area 17) and V2 (Brodmann area 18). V1 was also engaged when, instead of the old/new recognition task described above, participants were asked to first indicate if studied shapes originally appeared on the left or right of fixation and then were asked to indicate the level of confidence for their response on a three-point scale (i.e. "unsure", "sure" or "very sure"; Karanian & Slotnick, 2018). Specifically, researchers found activity in contralateral areas of V1 during both true (i.e., correct left/right mnemonic spatial judgements) and false memories (i.e., incorrect spatial judgements with "sure" or "very sure" confidence levels). The magnitude of activity for true memory was greater than false memory and their respective locations were in distinct sub-regions of V1. Further, the frequency of "very sure" false memories decreased when transcranial magnetic stimulation disrupted areas of V1 previously localized for false memory in the same paradigm.

Taken together, the evidence above suggests that ventral visual stream areas can be recruited during memory tasks that normally engage MTL, if the stimuli used in the task reside at an appropriate lower-level of complexity. Further, as described in the previous sections, MTL demonstrates functional versatility, being engaged during both perceptual and mnemonic tasks, and content-dependent mnemonic engagement of MTL sub-regions. Modern modular-based theories fail to account fully for the combination of these findings. However, a non-modular theory that redefines the role of regions in the

MTL and ventral visual stream in terms of the representations they contain, rather than the cognitive processes they support, can accurately capture the perception and memory findings above. A relatively recent theory called the representational-hierarchical (R-H) theory takes this approach.

1.5 Representational-Hierarchical Theory

The R-H account, as it applies to memory, was initially put forth as a connectionist model of object recognition memory in PRC (Cowell, Bussey, & Saksida, 2006). The model first assumes that neural representations of visual stimuli are organized by the complexity of the represented information (Bussey & Saksida, 2002; Cowell et al., 2006). Complexity is defined as the dimensionality of a representation (e.g. a color can be defined by three dimensions, but a face needs more than three dimensions to be uniquely specified). Further, the organization of neural representations by complexity unfolds across brain regions in a hierarchical manner (Figure 1). Posterior areas in ventral visual stream represent very simple features (e.g., the color pink, a line orientation), whereas more anterior regions in ventral visual stream first bring simple features together into simple conjunctions (e.g., a triangle, a pink circle), and later into complex conjunctions (e.g., pink circle on top of tan triangle with the semantic label of 'ice cream cone'). The hierarchy extends into MTL and culminates at HC, where it processes conjunctions of items within their spatial and/or temporal contexts (e.g., eating ice cream last week at the beach; Bussey & Saksida, 2002; Cowell et al., 2006; Kent, Hvoslef-Eide, Saksida, & Bussey, 2016). Each stage of the hierarchy has the capability to form

conjunctions of the representations contained at the previous stage, and thus each region is configural relative to earlier stages (Bussey & Saksida, 2002).

In the R-H model, the 'tuning' of neural activation patterns serves as a measure of familiarity (Cowell et al., 2006). That is, neural activation patterns for a representation become more selective each time a visual stimulus corresponding to that representation appears. Repeatedly presented, and thus familiar, stimuli elicit a peak of high activation (i.e., sharply tuned representations), while novel stimuli elicit a moderate level of activation, broadly distributed across the cortex (i.e., coarsely tuned representations). For example, the *neural representations* of a strawberry ice cream cone undergo neural tuning when a strawberry ice cream cone *stimulus* is presented during the study phase of an object recognition task. When the strawberry ice cream cone stimulus is re-presented at test, the neural activation patterns for the conjunction representation (i.e., a pink circle on top of a tan triangle), located in PRC, and the collection of individual feature representations (i.e., pink, tan, circle, triangle, etc. separately), located in posterior visual cortex, will both demonstrate neural tuning. This tuning will consequently signal the item as familiar for a correct mnemonic judgment.

However, neural tuning, signaling familiarity, can develop for feature representations in response to not only the presentation of attended, deliberately encoded stimuli, but also in response to interference. The R-H model assumes that all items in the visual world are composed from a limited pool of visual features, meaning that most common objects share features with some other objects. Therefore, in a memory task, the features of the objects that are presented at test may in fact appear repeatedly as part of visual stimuli in the surrounding environment (or even as part of "imagined" visual

stimuli) that are encountered between the study and test phase of the task. Critically, even novel stimuli that appear in the test phase will be composed of features from the same limited pool. The repeated encountering of the commonly occurring object features results in all such neural feature representations undergoing tuning, and thus eventually appearing familiar. Even individual feature representations of a *novel* object, housed in posterior visual cortex, become sharply tuned, and thus appear familiar at test. Consequently, if an individual must make mnemonic judgments using posterior feature representations alone, as is the case when conjunction representations are impaired following PRC damage, a novel object will be incorrectly judged as familiar.

Importantly, though, in the healthy brain mnemonic interference between intervening items during a delay and novel items can be resolved by a conjunction representation, which provides additional information about a stimulus beyond that contained in its feature representations (Cowell et al., 2006). Representations at the conjunction level are unique and selective for the exact conjunction they represent. It is very unlikely that the exact conjunction will be shared between intervening items and novel stimuli (because "whole" stimuli reside in a very high-dimensional space, where the same point, representing a unique object, is rarely drawn upon twice by chance). Thus, it is unlikely that the novel conjunction representation is tuned via the presentation of other visual stimuli. Consequently, the conjunction representation of a novel object, housed in anterior PRC, always appears novel. Here, the "whole" conjunction representation is "greater than the sum" of its component feature representations and is required for successful mnemonic discrimination.

The model can similarly explain the critical role of conjunction representations for object recognition memory tasks when familiar and novel stimuli are purposely designed to share many low-level features. Consider the presentation of a familiar strawberry ice cream, as described above, and a novel *mint* ice cream cone at test. This novel stimulus is represented, according to the R-H model of memory, at both the conjunction (i.e., a green circle on top of a tan triangle), PRC, level and feature, posterior visual cortex level (i.e., green, tan, circle, triangle, etc. separately). The familiar strawberry ice cream and the novel mint ice cream share many of the same neural feature representations (i.e., tan, circle, triangle, etc., separately), and these shared feature representations undergo tuning during presentation of the strawberry ice cream stimulus at study. Therefore, even though the particular conjunction of features comprising the novel mint ice cream is novel, the majority of its features — when considered in isolation — are not. Consequently, for individuals with PRC-lesions, whose mnemonic judgements must be made at the feature level alone (because conjunction representations in PRC are compromised), the sharply tuned features of a novel object signal familiarity, and a novel stimulus is incorrectly judged as familiar.

However, in a healthy brain, neural tuning at the conjunction level correctly signals novelty for novel stimuli. The conjunction representation of the strawberry ice cream undergoes tuning during the encoding phase, and thus signals familiarity at test. Conversely, because the exact conjunction of features is distinct between familiar stimuli and novel stimuli, the conjunction representation of the novel mint ice cream remains coarsely tuned, and thus provides an unambiguous signal of novelty at test.

Consequently, the novelty signal at the conjunction level overrides the familiarity signal at the feature level and the novel mint ice cream is correctly judged as novel.

Further, the R-H model proposes that memory and perception rely on a shared hierarchy of neural representations. Although the example above featured an *object recognition memory* task and signatures of familiarity, the same example could be given within the context of a *perceptual discrimination* task. That is, if the strawberry and mint ice cream cones were presented simultaneously, they would appear almost identical at the feature level because they are represented as two highly overlapping collections of simple features. However, at the conjunction level, the two stimuli remain perceptually distinct because the presence of even one non-shared feature entails that they are represented as two unique items that correspond to activation across two distinct neural patterns in PRC (Bussey & Saksida, 2002; Cowell et al., 2006).

Consequently, the cognitive function (e.g., memory or perception) thought to be involved during a task does not dictate engagement of brain areas; instead, the level of the representational hierarchy that best disambiguates the stimuli is key. If successful discrimination between two stimuli requires conjunction representations (i.e., if stimuli share many features), then the region containing conjunction representations (for most stimuli, anterior ventral visual stream, MTL) will be engaged. However, if successful discrimination can be made on the basis of individual feature representations alone (i.e., if stimuli do not share features), then the region containing feature representations (i.e., posterior ventral visual stream) will be engaged instead. Further, the specific conjunction and feature representations required will vary based on the complexity of the stimuli. That is, disambiguating similar scenes will require conjunction representations located

further anterior than the conjunction representations required to disambiguate similar objects (i.e., HC versus PRC; see Figure 1). Therefore, the R-H model predicts that all regions along the representational continuum can be involved in both memory and perception; a region's engagement is dependent on the representational demands of the task.

As outlined above, the R-H theory can explain (1) how MTL structures are involved in both perception and memory; (2) why engagement of MTL sub-structures varies by stimulus content; and (3) how ventral visual stream areas are involved in both perception and memory. But, the model does so by making three key assumptions regarding conjunction representations. First, structures along a pathway extending from the ventral visual stream into MTL (VVS-MTL pathway) are assumed to be organized in a hierarchical manner based on the conjunctive complexity of the representations they contain, such that conjunction representations of higher complexity are located in more anterior VVS-MTL pathway structures. Second, within this pathway, the "whole" conjunction representation is "greater than the sum" of its component feature representations and thus provides additional information to disambiguate similar stimuli. Third, the involvement of a brain region in a given task is determined by the representation required for that task, rather than which "cognitive process" is putatively required. In the next sections, I will review the evidence in support of these assumptions and will highlight the remaining gaps in the literature.

1.5.1. Evidence for a Representational Hierarchy

In the ventral visual stream, a hierarchical organization of representations has been featured in many existing models of vision (Desimone & Ungerleider, 1989; Hubel & Wiesel, 1965; Riesenhuber & Poggio, 1999) and is well supported with evidence from animal research. Early visual cortex demonstrates a preference for neural coding of lower-level simple features. For example, V1 in primary visual cortex is tuned to simple stimulus attributes, such as orientation and spatial frequency (Hubel & Wiesel, 1962, 1965; Mazer, Vinje, McDermott, Schiller, & Gallant, 2002) and V4 and posterior inferotemporal cortex demonstrate selectivity for moderately complex conjunctions, such as curvature, complex shapes, combinations of shape and texture/color, and stimulus invariance (T. Kim, Bair, & Pasupathy, 2019; Kobatake & Tanaka, 1994; Rust & DiCarlo, 2012; Yau, Pasupathy, Brincat, & Connor, 2013). The hierarchy transitions to preferential coding of complex conjunctions in structures located further anterior in the ventral visual stream, such that conjunction-coding for complex objects is seen in anterior inferotemporal cortex (Desimone, Albright, Gross, & Bruce, 1984; Desimone, Schein, Moran, & Ungerleider, 1985; Kobatake & Tanaka, 1994).

This representational hierarchy is further evidenced by findings from humans using fMRI methods (Wilson & Wilkinson, 2015). Selective coding for simple features, like orientations, occurs early in V1 (Kamitani & Tong, 2005; Serences, Saproo, Scolari, Ho, & Muftuler, 2009). This preference for features becomes more conjunctive in V2 where there is selectivity for the conjunction of form and color (Seymour, Clifford, Logothetis, & Bartels, 2010) and in V4 where there is selectivity for curved shapes (i.e., the conjunction of two simpler line orientations; Wilkinson et al., 2000). Coding preference for mid-level representations emerges in occipito-temporal cortex, as shown

with a novel stimulus set composed of object images that have been scrabbled to be unrecognizable while preserving some mid-level texture and form information (Long, Yu, & Konkle, 2018). Further, higher-level coding occurs for object category identity in lateral occipital cortex (LOC) and for faces in fusiform face area (Guggenmos et al., 2015; Haxby et al., 2001; Kanwisher et al., 1997).

Although this visual processing stream was initially thought to culminate in LOC and fusiform face area, recent evidence suggests that it continues into MTL. PRC demonstrates preferential coding for high-level conjunctive information used to distinguish highly similar objects (Erez, Cusack, Kendall, & Barense, 2015; Tyler et al., 2013), and the conjunction of specific objects with semantic information (Clarke & Tyler, 2014; Martin, Douglas, Newsome, Man, & Barense, 2018). Further, when stimuli were composed of person, object and scene 'features', only in PHC did neural data enable classification of conjunctive stimulus identities in the absence of significant feature information, despite searching in LOC and fusiform cortex (van den Honert, McCarthy, & Johnson, 2017). That is, as put forth by the R-H account (Bussey & Saksida, 2002), when the features of a stimulus were more complex, the conjunction of those features was found to be represented further along the VVS-MTL representational continuum, meaning conjunctions were not limited to a single region.

In addition to evidence for the dominance of feature-coding in earlier ventral visual stream areas and of conjunction-coding in later ventral visual stream and MTL areas, the existence of an explicit shift between the two coding types has been recently confirmed. Using a novel multivariate pattern analysis (MVPA) of fMRI data, Cowell et al. (2017) found evidence along the ventral visual stream for a transition from areas that

represent more information about lower-level features individually than information about their conjunction (i.e., feature-coding) to areas that represent more information about the conjunction of those features as whole objects than about the features individually (i.e., conjunction-coding). Participants were scanned while viewing a series of simple object stimuli composed of a conjunction of four features: left and right outline features and left and right spatial frequency features; each of the four features was binary meaning it could take on one of two values (see Figure 2 for complete stimulus set). Researchers used the brain data from those scans to train a set of classifiers, with the goal of the classifiers being to identify correctly either a specific feature or a specific stimulus that was viewed on a given trial, from the neural activation pattern. Four of the classifiers sought to determine the identity of each of the four separate features (i.e., which of the possible two values for a given feature was present) and a single object classifier sought to determine the identity of the whole unique conjunction (i.e., which of the sixteen objects was presented).

Two classification accuracies were then derived from regions along the ventral visual stream: (1) a *predicted* object-level classification accuracy that was the product of the four two-way feature-classifier accuracies; and (2) an *empirically observed* object-level classification accuracy that was the single accuracy of the 16-way conjunction-classifier. The predicted object accuracy was taken as a measure of the extent to which a brain region can identify the whole object *based only on a linear combination of the knowledge it contains about individual features*. The empirical object accuracy was taken as a measure of the extent to which a brain region contains information about the whole

object. These two classification accuracies were pitted against each other in a log-ratio, forming a feature conjunction index (FCI):

$$\mathrm{FCI} = \ln\left(\frac{Empirical\ object\ accuracy}{Predicted\ object\ accuracy}\right)$$

A positive FCI value indicated a conjunction-coding region and a negative FCI value indicated a feature-coding region. What emerged was a transition starting in ventral visual stream from V1, where FCI values were most negative (i.e., reflecting coding of feature information), to V2 and V3, where FCI values were less negative (i.e., reflecting coding of a mix of feature and conjunction information), to LOC and other occipito-temporal brain regions found via a searchlight analysis, where FCI values were numerically positive or in some cases statistically greater than zero (i.e. reflecting coding of conjunction information).

Taken together, the findings described above provide clear evidence for the emergence of conjunction representations in humans, as assumed by the R-H theory. Importantly, though, anterior ventral visual stream regions are not the only regions assumed to contain representations of conjunctions (Cowell et al., 2017). Within the R-H model, all levels contain conjunctions of the elements that were represented at earlier levels, such that early regions contain simpler conjunctions and later regions, including MTL, contain conjunctions that are more complex. Although some MTL voxels exhibited significant conjunction-coding, Cowell et al. were cautious to draw conclusions about preferential conjunction-coding in MTL structures because of the small numbers of significant voxels in these areas. It is possible that fewer MTL voxels were found to be significant because the stimuli in the study (2-D monochrome simple objects) did not contain the conjunctive complexity that is usually processed in those anterior areas. An

analogous study with more complex stimuli is warranted to establish whether conjunction-coding extends into MTL, as seen in Erez et al. (2015) and, importantly, if the transition point from feature-coding to conjunction-coding varies according to the conjunctive complexity of a stimulus set.

1.5.2. Evidence for the Importance of Task Representational Demands

Prior research has explored how task representational demands influence a brain structure's engagement. This has been most extensively investigated within the context of complex objects, and thus at the level of PRC within the representational hierarchy. As described previously, individuals with PRC-lesions show impaired performance during perceptual discrimination tasks when object features appear as part of both rewarded and unrewarded object stimuli (Barense et al., 2005; A. C. H. Lee, Barense, et al., 2005; see Section 1.2). Owing to the feature ambiguity present in these tasks, representations of each object as a distinct conjunction, as contained in PRC, are required to discriminate successfully between items. If PRC representations are compromised, discrimination judgements must be made using the remaining representations, in undamaged posterior regions, which correspond to lower-dimensional representations of individual features. However, at this level, objects are represented as a collection of highly similar features and are more difficult to disambiguate, thus leading to more errors.

Because, under the R-H account, perception and memory rely on a shared hierarchy of neural representations, if the representational demands of a *mnemonic* task are similar to those described in the perceptual task above (i.e., if feature representations alone provide only ambiguous information), the task will also require PRC conjunction

representations. Via neural tuning mechanisms, ambiguous feature-level familiarity signals (i.e., neural tuning of both familiar and novel feature representations) can result from interference or because novel and familiar objects are designed to inherently share many features. In both cases, feature representations belonging to *familiar* items will undergo neural tuning during the study phase. In the case of interference, feature representations belonging to *novel* items will undergo neural tuning when those features appear as part of visual objects during a delay between the study and test phases of a memory task. (At the feature-level, this is likely to occur because all objects, including objects selected as novel items in a memory test, are composed of features from a common and limited pool of possible features). In the case of shared features between familiar and novel stimuli, feature representations belonging to *novel* items will also undergo neural tuning, but when shared features appear as part of familiar objects during the study phase. Therefore, in both cases, both familiar and novel features demonstrate neural tuning, signaling familiarity, and feature representations alone provide only ambiguous mnemonic information.

A specific set of predictions follows for selective-PRC-lesion patient memory studies. When complex conjunction representations of objects are impaired, as in cases of selective PRC damage, an individual must rely upon familiarity signals from posterior feature representations alone. However, at the feature level, the novel object stimulus cannot be distinguished from the familiar object stimulus in terms of familiarity – the features of both stimuli (the familiar item and the novel item) undergo neural tuning and appear familiar.

Studies using implicit measures of memory with lesioned rats confirm the predictions of the model, and specifically the counter-intuitive prediction that when PRC lesions induce memory discrimination failure, they do so because novel objects appear familiar, rather than because familiar objects appear novel (Bartko et al., 2007b). In an initial sample phase, rats with bilateral PRC lesions were exposed to two identical objects made of Legos. In a second sample phase, the rats were exposed to another pair of identical Lego objects that were composed of different Lego pieces (i.e., features) than those used in the Sample 1 objects. In a final choice phase, the rats were exposed to the Sample 1 Lego object and one of two possible novel objects. Novel objects were either composed of (1) Lego pieces featured in Sample 1 and Sample 2 objects, but never seen together (i.e. familiar features, but novel conjunction of features), or (2) Lego pieces that did not appear in either of the sample phases (i.e., novel features and novel conjunction of features). In general, healthy rats spend more time exploring novel stimuli than previously encountered stimuli; accordingly, length of exploration period can serve as a measurement of familiarity. In this study, when novel Lego objects were composed of familiar features, lesioned rats demonstrated reduced exploration periods to novel stimuli, ostensibly treating novel objects as familiar.

This finding was extended to humans in a similar paradigm using eye fixations as a proxy for familiarity judgments (Yeung, Ryan, Cowell, & Barense, 2013). Healthy humans show more fixations towards novel stimuli than to previously encountered stimuli; thus, number of eye-fixations can be taken as a measure of familiarity that avoids contamination by verbal report and participant expectations, similar to “exploration time” in rodents. When many features are shared between familiar and novel stimuli, humans at

risk for mild cognitive impairment (a disorder that indicates likely incipient MTL damage; Petersen et al., 2006) demonstrated reduced eye-fixations to novel stimuli, seemingly treating novel objects as familiar. Again, the R-H account predicts these results because the features of the novel object (considered in isolation) bear neural signatures of familiarity via neural tuning of those feature representations when they previously appeared as part of seen objects. In the case of MTL damage, the representations needed to complete the task — conjunction representations of objects in which unique objects are represented distinctly — are impaired and discrimination judgements are dependent on feature representations alone. Thus, novel items with familiar features are judged to be familiar.

It would be incorrect to interpret the above evidence as support for PRC as a region that is uniquely critical for all recognition memory tasks. According to the R-H account, any recognition memory task is solved by the brain region that best disambiguates novel and familiar stimuli at test. In the case of an object recognition memory task where features appear as part of both familiar and novel objects, PRC is the region that best separates the unique conjunctions corresponding to an object. Further, it has also been suggested that HC may be so frequently implicated in episodic memory because it houses the conjunction representations that are most frequently required in episodic memory tasks (i.e., temporal and spatial contexts or associations between paired items; Cowell, Barense, & Sadil, 2019; Cowell et al., 2006). However, the R-H account predicts that if a mnemonic task instead tested recognition memory for 2-dimensional features, posterior areas that contain those feature representations would be critical for successful completion. Although the above findings demonstrate how a task's

representational demands specifically recruit PRC or HC for recognition memory, and although there is previous evidence for recognition memory signals in ventral visual stream, there has yet to be a direct demonstration of how manipulating representational demands within the same memory task can cause the locus of memory signals to vary between MTL and ventral visual stream regions.

1.6 Aims

The current experiment investigated outstanding questions in the literature supporting the R-H account. First, there is evidence for a transition from feature representations to conjunction representations, but this has only been demonstrated with a lower-level simple object stimulus set (Cowell et al., 2017). It is not only important to test the generalizability of this finding to other stimulus sets, but also to test the prediction of the R-H account that the locus of this transition point varies based on the conjunctive-complexity of a stimulus set.

The study phase (first scan session) of the current experiment examined this prediction by implementing the Cowell et al. (2017) paradigm with two stimulus sets of varying conjunctive-complexity: novel 3D objects, known as fribbles, and novel computer-generated scenes. That is, the present study aimed to find the cortical locus at which neural representations become less informative about individual features of a complex object (i.e. 3-D colored shapes) or complex scene (i.e., room shape, color and furniture) and more informative about the conjunction of those features. Additionally, the study sought to ascertain if this transition point varies between simpler stimulus sets (i.e.,

fribbles) and more complex stimulus sets (i.e., scenes). I predicted that the locus of the transition point would be further anterior for scenes than for fribbles (Prediction #1).

Second, the R-H theory claims that the involvement of a brain region during a task is determined by the representational demands of the task, and which region contains the representations that meet those demands. Under this assumption, the R-H theory has accounted for PRC's critical and selective role in memory for complex objects (Bartko, Cowell, Winters, Bussey, & Saksida, 2010; Bartko et al., 2007b; Cowell et al., 2006; Delhaye, Bahri, Salmon, & Bastin, 2019; Eacott et al., 1994; McTighe, Cowell, Winters, Bussey, & Saksida, 2010; Meunier et al., 1993; Yeung et al., 2013). However, to what extent the cortical locus of memory signals can be *made to vary* by direct manipulation of representational demands during a recognition memory task, remains unanswered.

The test phase (second scan session) of the current experiment examined the locus of recognition memory signals along the VVS-MTL pathway when manipulating task representational demands in two ways. First, as in the study phase, the conjunctive-complexity of stimuli was varied by using two stimulus sets of different complexity (fribbles and scenes). I predicted that memory signals for scenes would reside in further anterior sites than memory signals for fribbles (Prediction #2). Second, the type of information retrieved was assayed in a manner to reflect two types of memory, either retrieval of conjunction representations (i.e. conjunction memory) or retrieval of feature representations (i.e., feature memory). That is, the test phase aimed to find the cortical locus for conjunction memory and feature memory for both fribbles and scenes. I predicted that conjunction memory signals would reside further anterior than feature memory signals, for both stimulus sets (Prediction #3).

Finally, both phases of the experiment, for each stimulus set separately, were also used to investigate to what extent brain regions that evoked conjunction or feature memory-related activation *during retrieval* (second, "memory test" scan session) were the same brain regions that contained conjunction-coded or feature-coded neural representations for objects and scenes *during perceptual processing/encoding* (first, "study phase" scan session). I predicted that there would be some degree of anatomical correspondence between the type of neural coding and the type of memory signal, such that feature-coding sites exhibit feature-memory signals, and conjunction-coding sites contain conjunction-memory signals (Prediction #4). Testing these four predictions is a critical step in assessing the validity of the non-modular R-H account.

CHAPTER 2

EXPERIMENT

2.1 Overview and Predictions

In the first pair of scanning sessions – one for each stimulus set, fribbles and scenes, conducted on separate days – participants were asked to complete an incidental task (to ensure that they were awake and attending) while viewing a stream of fribble or scene stimuli. Both fribble and scene stimulus sets were created analogously to the stimuli from Cowell et al. (2017), such that any given stimulus was composed of the conjunction of three simple, binary features (see Figure 3, Figure 4 and Section 2.2.2. for more detail). According to the R-H theory, the transition from feature-coding to conjunction-coding found in Cowell et al. (2017) should be located further anterior, toward MTL, for stimuli that are more complex.

For fribbles, I expected posterior ventral visual stream areas and mid-ventral visual stream areas to contain feature-level codes. Feature-coding was expected to possibly extend to more anterior regions than the feature-coding regions found in Cowell et al. (2017). Compared to the features of Cowell et al.'s simple objects, the features in the fribble stimulus set could be represented at a similar posterior low-level (e.g., line orientation, color in early visual cortex), as well as at a more complex anterior mid-level (e.g., combinations of color and shape in V4). Additionally, the transition from feature-coding to conjunction-coding was expected to occur in object-selective anterior ventral visual stream and PRC.

Similarly, scenes are assumed to have more complex features than the features of fribbles. Thus, for scenes, I expected feature-coding to occur anywhere from posterior

ventral visual stream (for representations of low-level features, like line orientations and color) to mid-ventral visual stream areas and PRC (for mid-to-high-level features, like pieces of furniture). However, conjunction-coding of the entire scene stimulus was expected to occur in PHC and HC, alone.

In the second pair of scanning sessions, participants were asked to complete a recognition memory task based on the fribble or scene stimuli they had viewed in the first session (for each stimulus set, the first and second scan session occurred on the same day, but the two stimulus sets were tested on different days). In this test phase, trials belonged to one of three possible mnemonic classes: Novel, Recombination, and Familiar. On Novel trials, the individual features, as well as the conjunction of those features, had not been seen during the first session (i.e., both the features and the conjunction were novel). On Familiar trials, both the individual features and the exact conjunction of those features had been seen in the first session (i.e., both the features and the conjunction were familiar). However, on Recombination trials, the individual features had been seen as parts of items in the first session, but those features were conjoined in a novel way so that the whole item remained novel (i.e., the features were familiar, but the conjunction was novel).

By contrasting different pairs of trial types, we can assay different types of memory. That is because different pairs of trial types correspond to different levels of complexity in terms of the representation that provides a distinct familiarity signal between the two trial types being contrasted. A contrast of Novel and Recombination trials indexes feature memory because the familiarity of the individual features is the only factor that discriminates the two trial types (i.e., features are novel during Novel trials

and familiar during Recombination trials, whereas the conjunction is novel for both trial types). A contrast of Recombination and Familiar trials indexes conjunction memory because the familiarity of the conjunction of features is the only factor that discriminates the two trial types (i.e., features of both trial types are familiar, but the conjunction of Recombination trials is novel while the conjunction of Familiar trials is familiar).

According to the R-H theory, brain areas demonstrating signals for feature and conjunction memory are expected to coincide with the brain areas posited to contain feature and conjunction representations. The involvement of a region is not determined by the area's assumed cognitive function; it is determined by the *representational content* processed in a brain region and the necessity of that content to complete a task successfully. As such, the cortical locus of feature memory signals was expected to lie posterior to the locus for conjunction memory signals. Further, these two memory types (feature versus conjunction) may differ in location across stimulus sets, owing to differing conjunctive complexity between fribbles and scenes. Specifically, object-selective structures (i.e., LOC and PRC) were expected to be engaged for conjunction memory of fribble stimuli, and scene-selective structures (PHC, HC) were expected to be engaged for conjunction memory of scene stimuli. Additionally, early and mid-ventral visual areas were expected to be engaged for feature memory of fribble stimuli, and mid-ventral visual areas and posterior MTL structures were expected to be engaged for feature memory of scene stimuli.

Further, the current study aimed to provide a more direct measurement of the relationship between the location of representational content and the location of brain structures that are recruited for a mnemonic task. Therefore, in a searchlight analysis of

the study data, I defined feature-coding and conjunction-coding brain areas for scene and fribble stimulus sets, separately. Then, I conducted feature memory and conjunction memory contrasts of the corresponding fribble/scene test phase (memory-related) data within those stimulus-specific, functionally defined regions. I expected that signals for conjunction memory would be greatest in conjunction-coding brain areas and that signals for feature memory would be greatest in feature-coding brain areas.

2.2 Method

2.2.1 Participants

Twenty-three participants were recruited from the University of Massachusetts-Amherst community. All participants spoke English fluently; had normal or corrected-to-normal vision; had no history of neurological illness; and had no contraindications for MRI scanning. Participants were compensated $25/hour with an additional performance-based bonus up to $10 per scan session. Table 1 highlights when extreme outliers were identified and subsequently excluded from statistical analyses; for repeated-measures analyses all data points from a participant identified as an outlier were excluded.

2.2.2 Materials

Two different stimulus sets with different levels of complexity were created. The first set was composed of novel 3-D objects (i.e., fribbles) that were created using Strata Design 3D CX 7.5 (Barry, Griffith, De Rossi, & Hermans, 2014; Williams, 1998). Each individual fribble was a unique conjunction of three simpler features (3-D colored shapes referred to as “tail”, “body”, and “head” features) and each fribble belonged to a ‘family’ (see Figure 3). Within a given family, there were only two possible variants for each of

the tail, body and head features and those variants were unique to that family. Therefore, each family was composed of eight unique fribbles that were created using all possible conjunctions of a family's binary features. A total of four fribble families were created.

The second set was composed of novel 3-D scenes created using Sweet Home 3D, an indoor planning software. Analogous to the fribbles, each individual scene was a unique conjunction of three binary features (room shape, color and furniture) and each scene belonged to a 'family' (see Figure 4). Within a given family, there were two possible variants for each of the three room features and those variants were unique to that family. Consequently, each family comprised eight unique scenes that were created using all possible conjunctions of a family's binary room features. A total of four scene families were created.

Each subject was scanned twice on two separate days, once using fribbles as stimuli and once using scenes; stimulus set presentation order was counterbalanced across participants. In addition, each day's scanning involved two scan sessions – an initial, study phase scan session and a second, memory test phase scan session – which were separated by a short break. For a given stimulus set (fribbles/scenes), each participant was assigned two families to view in the first study phase, i.e., prior to the memory test, thus creating a number of stimuli designated as Familiar at test. A second class of test phase stimuli, Recombination stimuli, was created by combining two features of one Familiar family with a third feature of the other Familiar family (Figure 5). For these Recombination stimuli, although all of the individual features were seen as part of Familiar stimuli during the study phase, the conjunction of the features into these specific, unique wholes was never seen until the memory test. A final mnemonic stimulus

class, Novel stimuli, were created in the same manner as Recombination stimuli (i.e., 1 + 2 feature combination), but used features from the two remaining families that had not been designated as Familiar stimuli. Thus, for Novel stimuli, neither the individual features nor the unique whole were seen until the second memory test scan session. The assignment of particular families to stimuli classes (i.e., which two families were presented in the first scan session and which two families were reserved to create Novel stimuli at test) was counterbalanced across participants.

2.2.3 Task

Tasks were identical for fribble and scene stimulus sets. During study scans, participants were asked to complete a 1-back detection task (i.e., indicate if the stimulus currently on the screen is the same or different from the stimulus in the previous trial by pressing a button box response key). Additionally, there were 15 null trials randomly inserted between experimental trials. During the null trials, participants saw a white central fixation cross (+) that appeared to dim briefly by changing color to gray and back to white again. This 'dimming' occurred once or twice per null trial and participants were asked to press either response key whenever the dimming occurred. Participants did not need to make a 1-back detection response during experimental trials that immediately followed a null trial or occurred at the start of a scan. Before entering the scanner, participants first practiced this task on a laptop computer.

During the break between study and test scan sessions, participants received instructions on how to distinguish between the three mnemonic stimulus classes (i.e., Familiar, Recombination, and Novel). During test scans, participants were asked to indicate the stimulus class of the stimulus currently on the screen using three button box

response keys: (1) ‘Familiar’ (i.e., had been studied in the previous session); (2) ‘Recombination’ (i.e., was made of features that had been studied in the previous session, but now combined in a new way); or (3) ‘Novel’ (i.e., had not been studied in the previous session in any form). Null trials, as described above, occurred between each experimental trial. The instructions during the null trials remained the same.

For both study and test tasks, participants were instructed to respond while the stimulus was still on the screen and to be as accurate as possible. Participants were informed that a performance-based bonus was available based on both study and test scan session accuracy.

2.2.4 Experimental Design

The design was identical for fribble and scene stimulus sets. For a given stimulus set, each participant completed ten study and six test functional scans (Figure 6). During the scans, stimuli were displayed on a 32” LCD monitor positioned at the head end of the magnet bore. Participants were able to view the screen via a mirror on the head coil.

In the first, study scan session, stimulus presentation order was blocked across scans according to family (e.g., stimuli from one Familiar family were presented in even-numbered study scans and stimuli from the other Familiar family were presented in odd-numbered study scans), but randomized within a family block/scan. Within a single study scan, there were 35 stimulus trials, across which the eight stimuli from a Familiar family were presented sequentially on a gray background (each item repeated approximately four times, with three items being repeated a fifth time to create ‘immediate repeats’ that were removed from the analysis). Each study stimulus was presented for 2000ms and was immediately followed by a randomly assigned inter-stimulus interval (ISI) between

2000ms and 8000ms, during which a white central fixation cross appeared on a gray background. The response window for stimulus trials extended 1000ms into the ISI to ensure that participants had ample time to respond before the start of the next trial.

At least 500ms after the end of the response window, for 15 of the 35 ISIs within a single study scan, a null trial occurred. Null trials were restricted from occurring during ISIs less than 3000ms. For null trials during ISIs greater than 3000ms, but less than 6000ms, the white cross appeared as gray once, for 250ms. For null trials during ISIs greater than 6000ms, the white cross appeared as gray twice, each time for 250ms. The exact onset of the color change within the ISI was randomized within the constraints that color changes occurred at least 1000ms before the end of the ISI and there was at least 1500ms between two color changes in a single ISI. These null trials provided a behavioral measure of attention and wakefulness and also provided gaps in the stimulus sequence that allow for a better estimate of the hemodynamic response (HRF) for individual events. After completion of the 10 study scans, participants were given a self-paced break and exited the scanner before re-entering for the six test scans.

During the test scans, a total of 48 Novel, 48 Recombination and 48 Familiar stimulus trials were sequentially presented, such that 16 stimuli from each of the mnemonic stimulus classes were shown three times each. As stated earlier, Novel and Recombination stimuli were created by combining one feature of one family (either unstudied or studied for Novel and Recombination, respectively) with a third feature of the other unstudied/studied family. When implementing all possible 1 + 2 feature combinations, this design method allowed for the creation of 48 unique stimuli for both Novel and Recombination stimulus classes. However, because there were only 16 unique

Familiar stimuli, only a subset of 16 out of the 48 possible stimuli was selected for presentation at test for each of Novel and Recombination classes. Which 16 stimuli of the 48 were included in this subset was counterbalanced across participants.

Trial order and spacing of the three stimulus types was optimized using the easy-optimize-x MATLAB tool, which finds the most efficient design for later contrasting of conditions. Optimization was constrained such that the three stimulus types were equally distributed across the six test scans (i.e., eight of each stimulus type occurred in a scan) and that repetition was blocked (i.e., all 48 stimuli were shown for the first time before any stimulus was presented for a second time, etc.). Each test stimulus appeared for 2500ms, with a randomly assigned ISI between 4000ms and 12000ms. The response window for stimulus trials extended 1000ms into the ISI to ensure that participants had ample time to respond before the start of the next trial. All ISIs included a null trial, as described above, which did not commence until after the response window had elapsed (3500ms after stimulus trial onset).

All subjects were willing to repeat the experiment with the other stimulus set and returned on a separate day to do so, in order to avoid excessive fatigue and movement while in the scanner.

2.2.5 Image Acquisition

Scanning was performed on a Siemens 3T Skyra scanner equipped with a 64-channel head coil at the University of Massachusetts-Amherst's Human Magnetic Resonance Center. Functional images were acquired using a T2-weighted EP2D-BOLD sequence (TR: 1250ms; TE: 33ms; flip angle: 70^{o}; FOV: 210mm; $2.5mm^3$ voxels) and forty-two axial slices were acquired during each functional scan. Whole-brain anatomical

images were acquired in the middle of the study functional scan session using a T1-weighted MP-RAGE sequence (208 sagittal slices; TR: 2000ms; TE: 2.13ms; flip angle: 9^{o}; $1mm^{3}$ voxels).

2.2.6 fMRI Data Analyses

2.2.6.1 fMRI Data Preprocessing

Preprocessing was performed using fMRIPrep 1.5.2 (Esteban et al., 2019, 2018; RRID:SCR_016216), which is based on Nipype 1.3.1 (Esteban et al., 2018; Gorgolewski et al., 2011; RRID:SCR_002502). A full description of anatomical and functional data preprocessing steps, as automatically generated by fMRIPrep, is provided in AppendixAPPENDIX A. Functional data was co-registered to each individual's anatomical scan for a given session, high-pass filtered with a 128s cutoff, and transformed into standard space (MNI152NLin2009cAsym) for group-level searchlight analyses (functional data remained in native space for region of interest [ROI]-based analyses). Data used in univariate analyses (i.e., functional data from test scan sessions), also underwent smoothing with a 5mm FWHM Gaussian kernel. Following preprocessing, the data was analyzed with a combination of custom MATLAB scripts utilizing SPM 12 software and the CoSMoMVPA toolbox (Oosterhof, Connolly, & Haxby, 2016). Functional data from immediate-repeat trials during the study scan sessions and incorrect trials during the test scan sessions were omitted from all neuroimaging data analyses.

2.2.6.2 Definition of Regions of Interest

Each participant completed one localizer scan. During this scan, participants completed a 1-back detection task while viewing a series of black and white images of objects, scrambled objects, words, scrambled words, faces, and scenes. Trials were blocked by image category and each image was presented for 400ms with a 350ms ISI.

Ultimately, however, the localizer was limited in its ability to define only select ROIs (i.e., LOC, PHC) and probabilistic atlases were used instead to define ventral visual stream areas (i.e., V1, V2, V3, V3AB, hV4, ventral occipital cortex [VOC], LOC, temporal cortex [TOC]; Wang, Mruczek, Arcaro, & Kastner, 2015) and MTL areas (i.e., PHC, PRC, HC; Ritchey, Montchal, Yonelinas, & Ranganath, 2015). In all analyses, data from left and right hemispheres were combined into a single ROI. A subset of representative ROIs were selected for individual ROI analyses; this included V1, V2, V3, LOC, PHC, PRC, and HC. Because classifiers applied to individual ROIs located in MTL did not perform significantly above chance, for either the feature- or conjunction-level classification problems (Figure 7), larger regional ROIs were also created and used analogously in all ROI-based analyses. The motivation behind this choice was that the additional voxels in larger ROIs might provide additional information, if any is present in the neural activation patterns of these regions, and thus improve classifier accuracies. These regional ROIs included Early Ventral Visual Stream (VVS), composed of V1, V2, V3, and V3AB individual ROIs; Mid VVS, composed of hV4, VOC, LOC, and TOC individual ROIs; and MTL, composed of PHC, PRC and HC individual ROIs.

In addition to the probabilistically-defined individual and regional ROIs described above, a conjunction-coding and a feature-coding ROI for each stimulus set was defined to be used in the memory signal analysis. The definition of these ROIs avoids issues

related to circular analysis because the ROIs were functionally defined from study scan data, but were used in the analysis of entirely separate test scan data (Nikolaus Kriegeskorte, Simmons, Bellgowan, & Baker, 2009). The exact methodology used to define these ROIs is detailed below.

2.2.6.3 ROI-Based Analyses of Feature-Conjunction Index

The feature-conjunction index (FCI) analysis followed the methods described in Cowell et al. (2017). For each stimulus set, a separate general linear model (GLM) was estimated for each stimulus trial of the study phase, excluding immediate repeat trials (Mumford, Turner, Ashby, & Poldrack, 2012). Each of the 32 single-trial GLMs had one regressor for the trial, one regressor for all remaining trials, and six motion nuisance regressors. Each regressor combined a boxcar model of the study stimulus time-series with a canonical HRF. The model provided activation estimates for every voxel within an ROI for each trial separately. Estimates of the single-trial activation patterns (i.e., the activation estimates across all voxels within the ROI) for each ROI were then used in feature and conjunction classification analyses for each stimulus set.

For each of the two Familiar families of a stimulus set (corresponding to five scans of study phase data), a total of four non-probabilistic linear discriminant analysis (LDA) classifiers were trained using leave-one-run-out cross-validation: three 2-way feature-level classifiers and one 8-way conjunction-level classifier. This cross-validation approach involved training the classifier with activation patterns from four scans of 32 non-immediate-repeat trials and returning predicted conjunction or feature labels for the 32 trials of the remaining (held out) fifth scan. Predicted labels corresponded to the label

that had the highest discriminant score for a given trial. Note that the training sample contained data from only four scans, not nine, because the two Familiar families were blocked across scans, with each family appearing in five scans. This process was repeated five times so each of the five scans served as the test sample once.

For each trial across scans and for all classifiers, predicted labels were compared to target labels and scored 0 or 1 for incorrect versus correct classification. The three feature-level classification accuracies for a given trial were then multiplied together to provide a *predicted* conjunction classification accuracy (i.e., 0 or 1 for incorrect versus correct) for that trial based on classifying features alone. The *predicted* conjunction could only be correct if all three features were classified accurately. Both the *empirically observed* conjunction classification accuracy (i.e., 0 or 1 if the 8-way conjunction-level classifier predicted the correct label) and the *predicted* conjunction classification accuracy (i.e., the product of multiplying the 0's or 1's of the three 2-way feature-level classification accuracies) were averaged across trials.

The averaged *empirically observed* conjunction classification accuracy was then compared to the averaged *predicted* conjunction classification accuracy by taking the natural log of that ratio, and thus producing an FCI value. Positive FCIs indicate that activation within a region is modulated by conjunctions more than features and negative FCIs indicate that activation within a region is modulated by features more than conjunctions (Cowell et al., 2017). FCIs were averaged across the two Familiar families for each subject and this averaged FCI value served as the dependent measure in the ROI-based FCI analyses below.

2.2.6.4 ROI-Based Analyses of Memory Scores

For each stimulus set, a GLM was constructed with one regressor for each of four conditions: correct responses to Familiar, Recombination and Novel stimulus types; and incorrect responses. Six motion nuisance regressors were also included in the model. Each regressor combined a boxcar model of the test stimulus time-series with a canonical HRF. For each subject, the model provided activation estimates, or beta weights (β) for every voxel within an ROI, for each of the four conditions. The beta weights for correct Familiar, Recombination and Novel stimulus types were used in obtaining indices of feature and conjunction memory.

Memory signal indices were derived by defining two contrasts, which are defined in equations at the end of this section. I will first describe, conceptually, how these scores are defined. To index feature memory, the beta weights from Novel and Recombination correct trials were contrasted (i.e., a memory signal that likely emerges on the basis of features, because the *features* are familiar in Recombination stimuli but novel in Novel stimuli, whereas the *conjunctions* are mostly novel in both the Recombination and Novel stimuli). To index conjunction memory, the beta weights from Recombination and Familiar correct trials were contrasted (i.e., a memory signal that must stem from conjunctions, because the *conjunctions* are novel in Recombination stimuli but familiar in Familiar stimuli, whereas individual *features* are familiar in both stimulus types). In the case of feature memory, the resulting beta weight estimates from the GLM for correct Recombination trials ($\beta_{Recombination}$) were subtracted from beta weight estimates for correct Novel trials (β_{Novel}). In the case of conjunction memory, the beta weight estimates for correct Familiar trials ($\beta_{Familiar}$) were subtracted from the beta weight estimates for correct Recombination trials ($\beta_{Recombination}$).

For both contrasts, the mean difference averaged across voxels within an ROI was then divided by the standard deviation of that difference to obtain a directional Cohen's *d* statistic. Calculating effect sizes allows for comparisons of the magnitude of effects across ROIs with different numbers of voxels and different signal-to-noise levels. These effect sizes are referred to as feature memory scores (from the Novel versus Recombination contrast) and conjunction memory scores (from the Recombination versus Familiar contrast):

$$Feature\ Memory\ Score = Cohen's\ d_{\ Feature} = \frac{\bar{x}_{\beta_{Novel} - \beta_{Recombination}}}{sd_{\beta_{Novel} - \beta_{Recombination}}}$$

$$Conjunction\ Memory\ Score = Cohen's\ d_{\ Conjunction} = \frac{\bar{x}_{\beta_{Recombination} - \beta_{Familiar}}}{sd_{\beta_{Recombination} - \beta_{Familiar}}}$$

Where $\beta_{Novel} - \beta_{Recombination}$ is a subscript that refers to the difference of two vectors: β_{Novel} refers to a vector of beta weights derived from all voxels in a given ROI on "Novel" trials in which the participant responded correctly (incorrect trials were removed from the analysis); and $\beta_{Recombination}$ refers to a vector of beta weights for all voxels in the same ROI on "Recombination" trials in which the participant responded correctly. Thus, $\bar{x}_{\beta_{Novel} - \beta_{Recombination}}$ is the mean value for the $\beta_{Novel} - \beta_{Recombination}$ difference vector, averaged across all voxels in the ROI, and $sd_{\beta_{Novel} - \beta_{Recombination}}$ is the standard deviation of the $\beta_{Novel} - \beta_{Recombination}$ difference vector calculated across all voxels in the ROI. Analogously, the $\beta_{Recombination} - \beta_{Familiar}$ subscript refers to the difference of two vectors: $\beta_{Recombination}$ refers to a vector of beta weights derived from all voxels in a given ROI on "Recombination" trials in which the participant responded correctly; and $\beta_{Familiar}$ refers to a vector of beta weights for all voxels in the same ROI

on “Familiar” trials in which the participant responded correctly. Thus, $\bar{x}_{\beta_{Recombination} - \beta_{Familiar}}$ is the mean value for the $\beta_{Recombination} - \beta_{Familiar}$ difference vector, averaged across all voxels in the ROI, and $sd_{\beta_{Recombination} - \beta_{Familiar}}$ is the standard deviation of the $\beta_{Recombination} - \beta_{Familiar}$ difference vector calculated across all voxels in the ROI.

2.2.6.5 Searchlight Analysis of the Intersection of Representational Content and Memory Signals

The above analyses produced two primary indices per stimulus set: FCI scores from the study phase scan session and memory scores (both feature and conjunction) from the test phase scan session. The R-H account predicts that because conjunction memory (i.e., the contrast of Recombination versus Familiar trials) requires conjunction representations to disambiguate seen and unseen stimuli, conjunction-coding regions should be engaged more than feature-coding regions for this contrast. Similarly, because feature memory (i.e., the contrast of Novel versus Recombination trials) can rely solely on feature representations for successful mnemonic discrimination, feature-coding regions should show a greater effect than conjunction-coding regions for this contrast.

To explore this prediction, conjunction-coding and feature-coding ROIs were defined via a searchlight analysis of the study scan data (Kriegeskorte, Goebel, & Bandettini, 2006). For each stimulus set separately, FCI was recorded at the center voxel of a spherical ROI (radius 5 functional voxels), defined as sets of neighboring voxels, throughout the brain. The group average of the spherical ROIs was calculated by averaging over subjects’ FCI values at each voxel, in normalized space. A group-level *t*-

test at each voxel was then used to compare the group mean FCI to zero. This comparison was used to define brain regions that demonstrated statistically reliable extremes of feature-coding (i.e., negative FCI values significantly less than zero) or conjunction-coding (i.e., positive FCI values significantly greater than zero). I then calculated conjunction and feature memory scores obtained from the corresponding fribble/scene test scan data within the stimulus-specific negative and positive FCI-ROIs defined by the study scan data.

2.3 Results

2.3.1 Behavioral Analysis

Performance during the study scan session indicated that participants stayed awake and successfully completed the incidental one-back detection task, in which participants indicated 'same' if the stimulus on the previous trial was the same as on the current trial, or 'different' otherwise. Discriminability between 'same' and 'different' trials, as measured by *d'*, was calculated by finding the difference between the normalized proportions of hits (i.e., trials when participants responded 'same' and the trial was 'same') and false alarms (i.e., trials when participants responded 'same' and the trial was 'different'). A large positive *d'* value indicates a greater percentage of hits and a lower percentage of false alarms, and thus better overall performance. The mean *d'* score was 3.21 and 3.26 for the fribble and scene stimulus sets, respectively. Performance did not significantly differ between stimulus sets, t (22) = -0.26, p = 0.8.

Behavioral performance on the recognition memory task during the test scan session was also measured with *d'*, which indexed the discriminability of the three classes of mnemonic status that were present among the test stimuli: Familiar, Recombination, Novel. Because there were more than two possible responses on a given trial, *d'* scores were calculated for each possible pairwise comparison of trial types. In each case, trials containing stimuli belonging to the third outstanding trial type were removed from the analysis. Any (erroneous) responses to the two trial types under comparison that invoked the outstanding trial type were binned as either a hit or a false alarm depending on the comparison. For example, in one comparison between Familiar and Novel trials, trials whose true status was Recombination were removed, and on the remaining trials (true status Familiar and Novel) any "Recombination" response was considered a hit on a Familiar trial, but a false alarm on a Novel trial. In a second comparison of the same two trial types (Familiar and Novel), a "Recombination" response was considered a false alarm on Familiar trials, but a correct rejection on Novel trials.

Table 2 shows the average *d'* scores for all such comparisons; overall, memory discrimination performance was good. Performance did not differ significantly between stimulus sets ($p = 0.53$), but did differ significantly between different pairwise comparisons (F [1.27, 26.57] = 89.07, $p < 0.001$). Unsurprisingly, *d'* scores were lowest, but still above chance, in the comparison of Familiar and Recombination trials (Novel responses treated similar to Recombination responses); these two trial types both contained stimuli in which all features of the stimuli were familiar from the study scan session, which would increase the difficulty of mnemonic discrimination.

2.3.2 ROI-Based Analyses of Feature-Conjunction Index

Although classifier accuracy was not of primary interest, for descriptive purposes mean classifier accuracies for both individual and regional ROIs, and fribble and scene stimulus sets are presented in Figure 7. Accuracy was lowest in MTL areas (PHC, PRC, HC) where the BOLD signal has a lower signal-to-noise ratio (SNR; Olman, Davachi, & Inati, 2009). A general guide for classifier chance performance was determined with a binomial test for two-way feature and eight-way conjunction classifiers, uncorrected for multiple comparisons. Classifier performance did not improve above this binomial chance threshold in MTL regions when using regional ROIs in place of individual ROIs. Because FCIs derived from classifiers performing at or below chance tend toward zero (Cowell et al., 2017), we should be cautious when interpreting the FCI results in these MTL areas. It is possible that zero FCIs are a reflection of 'hybrid' coding (i.e., areas that demonstrate a mixture of feature- and conjunction-coding), but, in the absence of reliably above-chance classifier accuracy, zero FCIs could also reflect regions that contain neither feature nor conjunction knowledge.

However, for regions outside of MTL with reliably above chance classifier performance, regional variation in SNR is much less likely to account for the FCI results described below. That is, we cannot infer that earlier regions have greater feature-coding than MTL regions simply because of greater SNR in those regions. Because the FCI measure places evidence for feature- and conjunction-coding into a ratio, both aspects of the measure should be similarly affected by noise within an ROI; at a minimum, simulations have shown that significantly negative FCI values can be produced only by a feature-based code and significantly positive values can be produced only by a conjunction-based code (see Cowell et al., 2017).

First, a two-way (2x7) ANOVA of FCI with factors of stimulus set (fribbles and scenes) and individual ROI (V1, V2, V3, LOC, PRC, PHC, HC) revealed a main effect of ROI, F (6, 126) = 4.41, $p < 0.001$, $\eta^2_G = 0.08$. Because there was no significant interaction of stimulus set and individual ROI ($p = 0.06$, $\eta^2_G = 0.04$), nor a main effect of stimulus set ($p = 0.51$, $\eta^2_G = 0.002$), this analysis was followed with a one-way ANOVA of individual ROI on FCI values that were averaged across stimulus set (Figure 8, top panel; though see Appendix B, top panels for FCI values separated by stimulus set). In this follow-up analysis, the main effect of ROI was still significant, F (6, 132) = 3.94, $p < 0.001$, $\eta^2_G = 0.13$, indicating that FCI values differed between individual ROIs. V1 and V2 located in early ventral visual stream areas had significantly negative FCI values (two-tailed *t*-tests Bonferroni corrected for seven comparisons, FCI = -0.08, $p = 0.004$; and FCI = -0.1, $p = 0.0002$, respectively) and FCI values became numerically positive, though not significantly so, in MTL areas PHC (FCI = 0.02) and PRC (FCI = 0.01).

An analogous analysis was completed with larger "regional" ROIs (Early VVS, Mid VVS, and MTL). A two-way (2x3) ANOVA of FCI again revealed a main effect of ROI, F (1.43, 30) = 6.64, $p = 0.008$, $\eta^2_G = 0.12$, but the interaction between stimulus set and ROI ($p = 0.73$, $\eta^2_G = 0.005$) and the main effect of stimulus set ($p = 0.91$, $\eta^2_G < 0.001$) were non-significant (see Appendix B, bottom panels for FCI values separated by stimulus set). Collapsing over stimulus set, a one-way ANOVA of ROI on averaged FCI values was significant, F (1.44, 31.71) = 8.09, $p = 0.004$, $\eta^2_G = 0.22$ (Figure 8, bottom panel). Both Early and Mid VVS ROIs had significantly negative FCI values (two-tailed *t*-tests Bonferroni corrected for three comparisons, FCI = -0.06, $p = 0.001$; and FCI = -

0.08, $p = 0.003$, respectively) and FCI values became numerically positive, though not significantly so, in MTL (FCI = 0.04).

2.3.3 ROI-Based Analyses of Memory Scores

Analyses were first performed within individual ROIs. Memory score, as measured by Cohen's D, served as the dependent variable in a three-way (2x7x2) ANOVA with factors of stimulus set (fribbles and scenes), ROI (V1, V2, V3, LOC, PRC, PHC, HC) and memory score type (feature memory and conjunction memory; see Appendix C, top panels for memory scores separated by stimulus set). There was a main effect of ROI, F (2.32, 46.32) = 17.87, $p < 0.001$, $\eta^2_G = 0.14$, and memory score type, F (1, 20) = 84.75, $p < 0.001$, $\eta^2_G = 0.36$, as well as an interaction between these two factors, F (2.37, 47.32) = 28.4, $p < 0.001$, $\eta^2_G = 0.19$. However, contrary to our prediction, there was no main effect of stimulus set or any interactions with stimulus set and other factors ($p > 0.05$, $\eta^2_G < 0.006$). Consequently, memory scores were once again averaged across stimulus sets in a follow-up two-way (7x2) ANOVA.

The follow-up analysis revealed main effects of memory type, F (1, 18) = 73.6, $p < 0.001$, $\eta^2_G = 0.47$, and ROI, F (2.26, 40.72) = 17.56, $p < 0.001$, $\eta^2_G = 0.22$, as well as an interaction between memory type and ROI, F (2.27, 40.9) = 35.6, $p < 0.001$, $\eta^2_G = 0.30$ (Figure 9, top panel). I explored this interaction further by separating the data for feature and conjunction memory and performing two one-way ANOVAs. This revealed a significant main effect of ROI in both cases (feature memory: F [2.4, 43.2] = 32.59, $p < 0.001$, $\eta^2_G = 0.48$; conjunction memory: F [2.44, 43.84] = 3.41, $p = 0.03$, $\eta^2_G = 0.08$). The greatest signal for feature memory occurred in individual ROIs located in early ventral visual stream (i.e., V1, V2, V3) and this signal decreased moving anteriorly to individual

ROIs located in MTL. Additionally, the greatest signal for conjunction memory occurred in individual ROIs located in MTL (i.e. PHC, PRC, HC) and late-stage ventral visual stream (i.e., LOC), and decreased moving posteriorly to individual ROIs located in early ventral visual stream. Conjunction memory was significantly positive in PRC (one-tailed *t*-tests Bonferroni corrected for four comparisons[2], Cohen's D = 0.16, $p = 0.01$), but was not different from zero in any other ROIs that demonstrated numerically positive scores.

The memory score effects found within individual ROIs were mirrored in the analyses within regional ROIs. A three-way (2x3x2) ANOVA of memory score revealed a main effect of regional ROI, F (1.46, 30.76) = 21.56, $p < 0.001$, $\eta^2_G = 0.11$, and memory score type, F (1, 21) = 81.2, $p < 0.001$, $\eta^2_G = 0.40$, as well as an interaction between these two factors, F (1.34, 28.16) = 35.21, $p < 0.001$, $\eta^2_G = 0.15$. All other effects were non-significant ($p > 0.05$, $\eta^2_G < 0.005$) and thus memory score was again averaged over stimulus set before any further analyses of these regional ROIs (see Appendix C, bottom panels for memory scores separated by stimulus set).

Collapsing over stimulus set, a two-way (3x2) ANOVA revealed a main effect of memory score type, F (1, 20) = 81.07, $p < 0.001$, $\eta^2_G = 0.54$, ROI, F (1.49, 29.72) = 18.75, $p < 0.001$, $\eta^2_G = 0.16$, as well as the interaction between these two factors, F (1.35, 27.06) = 31.22, $p < 0.001$, $\eta^2_G = 0.22$ (Figure 9, bottom panel). To explore this interaction further, two one-way ANOVAs for feature and conjunction memory scores were carried out separately. For feature memory, there was a significant main effect of ROI, F (1.46,

[2] In contrast to feature memory scores, conjunction memory scores clustered near zero. The goal of this series of statistical tests was to determine whether there was any reliable indication of conjunction memory, as measured by conjunction memory scores that significantly exceeded zero. Out of the seven individual ROIs, only four ROIs (LO, PHC, PRC, HC) had numerically positive conjunction memory scores. Therefore, comparisons, and the subsequent corrections for multiple comparisons, were implemented for these four individual ROIs only.

29.22) = 30.11, $p < 0.001$, $\eta^2_G = 0.38$. Compared to MTL, feature memory scores were greater in Early VVS, t (20) = 5.55, $p < 0.001$, and in Mid VVS, t (20) = 6.16, $p < 0.001$, but the two VVS regional ROIs did not significantly differ from each other, t (20) = 1.27, $p = 0.22$. For conjunction memory, there was a borderline main effect of ROI, F (1.32, 26.38) = 3.23, $p = 0.07$, $\eta^2_G = 0.05$. Compared to Early VVS, conjunction memory scores were significantly greater in Mid VVS, t (20) = -3.51, $p = 0.002$, and numerically, but not significantly, greater in MTL, t (20) = -1.97, $p = 0.062$. Conjunction memory did not significantly differ between Mid VVS and MTL regional ROIs, t (20) = -0.44, $p = 0.66$. Although signals for conjunction memory were numerically positive in both Mid VVS (Cohen's D = 0.13) and MTL (Cohen's D = 0.17), scores were significantly positive in only MTL (one-tailed t-tests, Bonferroni corrected for two comparisons[3], $p = 0.02$).

2.3.4 Searchlight Analysis of the Intersection of Representational Content and Memory Signals

In contrast to the individual and regional ROI-based analyses above, where FCI values and memory scores were averaged across fribble and scene stimulus sets, FCI-ROIs were defined *separately* for each stimulus set; the motivation for this decision is as follows. First, in terms of our theory, I did not expect to find stimulus-invariant negative and positive FCI regions (i.e., regions that were 'universal conjunction-coders' that

[3] Similar to the individual ROI analysis, conjunction memory scores within regional ROIs clustered near zero. Therefore, it was again important to determine whether there was any reliable indication of conjunction memory, as measured by conjunction memory scores that significantly exceeded zero. Out of the three regional ROIs, only two ROIs (Mid VVS, MTL) had numerically positive conjunction memory scores. Therefore, comparisons, and the subsequent corrections for multiple comparisons, were implemented for these two regional ROIs only.

yielded the strongest evidence for conjunctions for both fribbles and scenes), so constraining the searchlight analysis to such "shared" ROIs is not warranted *a priori*. Second, the fact that I found no stimulus set related differences in the FCIs and memory scores, and no stimulus set by ROI interactions in the *a priori* individual and regional ROIs above, does not necessarily entail that we should expect the same regions of the brain to contain the highest positive and lowest negative FCIs for the two stimulus sets. Lastly, evidence for stimulus set-related differences may have been masked in the individual and regional ROI-based analyses above. That is, there may in fact be differences between fribbles and scenes, but only in terms of the cortical locus for *conjunction* representations. In fact, where I predicted stimulus sets to differ the most in terms of FCI was within individual MTL regions. This possibility is explored below.

To further probe the data for any differences between FCI values due to the two stimulus sets, I performed an analysis of FCI restricted to individual ROIs located within MTL (i.e., PHC, PRC, HC). There was a significant interaction between stimulus set and ROI, F (2, 42) = 3.35, p = 0.045, η^2_G = 0.05 (Figure 10). The most positive FCI score was found within PRC for fribbles and within PHC and HC for scenes. This finding is in line with previous evidence of stimulus content coding specificity in MTL and my initial prediction. When defining positive FCI-ROIs via searchlight, similar stimulus set-related differences in the voxels identified may occur. Therefore, the decision to define FCI-ROIs separately for fribble and scene stimulus sets was well motivated.

The FCI-ROIs for fribble and scene stimulus sets are displayed in Figure 11. The coordinates for the ten most negative and ten most positive FCI-voxels included in the memory score analysis, and the general areas where these coordinates fell within the

Harvard-Oxford probability atlas (distributed with FSL, Smith et al., 2004), are listed for each stimulus set in Table 3 and Table 4. Fribble and scene stimulus sets contained a similar number of voxels in their respective negative and positive FCI-ROIs. For fribbles, the negative FCI-ROI consisted of 5194 voxels and the positive FCI-ROI consisted of 1544 voxels. For scenes, the negative FCI-ROI consisted of 6088 voxels and the positive FCI-ROI consisted of 1173 voxels. Between the two stimulus sets, although 1948 voxels were shared between negative FCI-ROIs, only 55 voxels were shared between positive FCI-ROIs.

For the fribble dataset, a two-way (2x2; [feature memory, conjunction memory] x [negative FCI-ROI, positive FCI-ROI]) ANOVA of memory score revealed an interaction between memory score type and ROI, F (1, 22) = 23.94, $p < 0.001$, $\eta^2_G = 0.16$, as well as main effects of memory score type, F (1, 22) = 17.89, $p < 0.001$, $\eta^2_G = 0.18$, and ROI, F (1, 22) = 17.55, $p < 0.001$, $\eta^2_G = 0.17$ (Figure 12, left panel). The same effects were found in the analogous two-way (2x2) ANOVA of memory score with the scene dataset (Type x ROI interaction: F [1, 20] = 11.49, $p = 0.003$, $\eta^2_G = 0.16$; Type: F [1, 20] = 26.17, $p < 0.001$, $\eta^2_G = 0.28$; ROI: F [1, 20] = 9.01, $p = 0.007$, $\eta^2_G = 0.06$; Figure 12, right panel). For both stimulus sets, feature-coding regions (i.e., negative FCI-ROIs) had greater feature memory signals than conjunction-coding regions (i.e., positive FCI-ROIs; fribbles: t [22] = 5.59, $p < 0.001$; scenes: t [20] = 3.96, $p < 0.001$). For scenes but not for fribbles, conjunction memory scores were numerically (but not significantly) greater in the positive FCI-ROI (Cohen's D = 0.15) than in the negative FCI-ROI (Cohen's D = -0.07). However, for both stimulus datasets, conjunction memory scores did not significantly differ from zero ($p > 0.05$) in either positive or negative FCI-ROIs.

CHAPTER 3

DISCUSSION

In the present experiment, there were two distinct behavioral phases, study and test, each associated with a separate MRI scan session; together, these two phases allowed me to test four predictions stemming from the R-H account of cognition. In the study phase, I attempted to extend the recent finding of a transition point from feature-coding to conjunction-coding regions, which was made using lower-level simple objects (Cowell et al., 2017), to two stimulus sets with greater conjunctive-complexity. That is, I sought to test for these more complex stimuli whether, when moving anteriorly along a theorized VVS-MTL pathway, a preference for coding information about an item's *individual features over the conjunction of features* would shift to a preference for coding information about an item's *unique conjunction of features over the individual features* themselves.

Additionally, I investigated whether manipulating the assumed complexity of a stimulus set would change the locus of this transition point. Specifically, in Prediction #1, I hypothesized that this transition point would be located further anterior for scenes than for fribbles owing to greater conjunctive-complexity among scenes than for fribbles. For fribbles, feature-coding was expected in posterior to mid-ventral visual stream areas, with a transition to conjunction-coding in object-selective LOC and PRC. However, for scenes, because both the features and conjunctions of scenes were assumed to be more complex than their respective fribble counterparts, I expected feature-coding to be located in posterior ventral visual stream to early MTL areas, with the transition to conjunction-coding also occurring later, in scene-selective PHC and HC.

Regarding Prediction #1, I did not find sufficient evidence that the relative preference for feature-coding or conjunction-coding, as measured by FCI, varied by the complexity of stimulus sets. Fribble and scene stimuli did not elicit significantly different FCI values in either the individual or regional ROI-based analyses. It is possible that the 'features' measured in this analysis captured low-level features (e.g. line orientation or color) – for which representations are expected to reside in early ventral visual stream areas for *both* stimulus sets – rather than mid-to-high-level features (e.g. colored shapes or furniture) – for which the stimulus sets diverged in complexity and thus for which the representations could be expected to reside at different points in cortex. Although the design of the two stimulus sets here aimed to manipulate 'features' at this mid-level (e.g., fribbles differed from one another by swapping 'head', 'body' and 'tail' features whereas scenes differed by swapping features that were whole objects like a bed or a sofa), mid-level and low-level features were conflated. For example, two mid-level 'body' features of a fribble always differed in terms of low-level features, like color, meaning the features could be discriminated on the basis of low-level visual properties or mid-level visual properties.

In support of this explanation, while the stimulus sets did not appear to differ in the locus of feature-coding, they did significantly differ in where the emergence of late-stage conjunction-coding began to occur. When the FCI analysis was limited to individual MTL sub-structures, PRC had the greatest tendency toward conjunction-coding (most positive FCI values) for fribbles and PHC and HC had the greatest tendency toward conjunction-coding for scenes. This pattern aligns with much previous data suggesting that PRC is preferentially recruited for object processing and PHC and HC are

more often engaged in scene processing (for review, see Robin, Rai, Valli, & Olsen, 2019). Therefore, I speculate that any evidence for a difference between stimulus sets may have been masked in the current study by common cortical loci for feature representations in their simplest form. Further investigation into whether the locus of mid-level conjunction codes varies when mid-level conjunction complexity is manipulated but low-level feature properties are held constant (i.e., thus, requiring *mid-level*, rather than *low-level* feature representations for successful feature identification during classification) is warranted. This would elucidate whether the present null result reflects a true lack of difference in the location of conjunction-coding for the two stimulus sets, rather than simply a lack of power in this experiment.

After I collapsed the data across stimulus sets, I found a transition from feature-coding (i.e., negative FCIs) to either 'hybrid' feature- and conjunction-coding (i.e., zero FCIs) or conjunction-coding (i.e., positive FCIs) when moving anteriorly along the VVS-MTL pathway. As predicted by the R-H account, posterior regions (i.e., V1, V2 among individual ROIs and Early and Mid VVS among regional ROIs) contained more information about individual features than the conjunctions of features.

Although anterior regions (i.e., PHC and PRC among individual ROIs and MTL among regional ROIs) contained numerically positive FCIs, I am cautious to present this finding as strong evidence that these regions contain more information about the conjunction of features than about individual features. That is because the FCI values in these regions were not significantly greater than zero and classifier accuracies for these regions were, on average, below the binomial threshold that I used as a heuristic to judge whether a classifier picked up sufficient information to perform above chance. As

mentioned earlier, FCIs derived from classifiers performing at or below chance tend toward zero (Cowell et al., 2017). Consequently, the FCIs captured in MTL areas could reflect hybrid coding, but could also reflect the absence of both feature and conjunction knowledge. To attempt to exclude the latter option, future investigations could implement techniques to improve classifier performance (e.g., including more trials in the experimental design, which would provide more trials for the classifiers to train on), or increase the power to capture statistically significant effects in MTL (e.g. increase sample size). Despite the inconclusiveness of MTL region analyses, the results of the present study still extend one finding of Cowell et al. (2017) to two new stimulus sets: visual feature information is best represented in posterior areas of the ventral visual stream.

The test phase of the experiment explored whether the locus of memory signals could be made to vary along the VVS-MTL pathway by manipulating the representational demands of a recognition memory task. According to the R-H account, engagement of a brain structure is not determined by whether a task requires a particular cognitive function (e.g., memory versus perception) and whether that function is localized to that structure. Rather, engagement of a brain structure is determined by what level of representation is needed to complete the task (e.g. fribble versus scene; feature versus conjunction) and whether that representation resides within that structure. Because I predicted that fribble and scene stimuli would vary in the cortical location of their respective feature and conjunction representations (Prediction #1), I additionally expected the locus of memory signals to vary by stimulus set (Prediction #2), such that the locus of memory signals would be further anterior for scenes than for fribbles.

Further, in Prediction #3, I hypothesized that signals reflecting conjunction memory (i.e., when the difference between two contrasted trial types [Recombination versus Familiar trials] was defined by a difference in familiarity for the conjunction of features) would be found in anterior ventral visual stream and MTL regions thought to house conjunction representations. Analogously, and more controversially, I predicted that signals reflecting feature memory (i.e., when Novel versus Recombination trials were contrasted, which differed in terms of feature familiarity alone) would be localized to posterior ventral visual stream regions thought to contain feature representations, and outside of traditional MTL 'memory areas'. The combination of Predictions #2 (a shift in memory signals for fribbles versus scenes) and #3 (a shift in memory signals for features versus conjunctions) led to specific expectations of PRC engagement during conjunction memory for fribbles, in contrast to PHC and HC engagement during conjunction memory for scenes. For feature memory, I expected early to mid-ventral visual areas to be engaged for fribbles and mid-ventral visual to posterior MTL areas to be engaged for scenes.

I did not find evidence for Prediction #2: memory scores did not differ significantly between fribble and scene stimulus sets, regardless of memory score type (feature versus conjunction) or ROI selection (small ROIs versus larger, regional ROIs). Similar to the FCI analysis, this could be due to a misspecification of what classifies as a 'feature', such that the features needed in the current paradigm may have resided at the earliest levels of the representational hierarchy and thus 'feature memory' appeared in identical cortical locations for both fribbles and scenes. Further, when considering conjunction memory, according to the R-H account, the distance between fribbles and

scenes is not predicted to be great: both stimulus sets would be expected to elicit memory signals for the conjunctions that comprise them within the MTL, in adjacent structures. The measure that I used to assess conjunction memory – the contrast between Recombination and Familiar trials – was perhaps an inherently weak signal, in line with the fact that the discrimination is subtle and behaviorally difficult to make. It is therefore possible that the current experiment lacked the statistical power to detect this small anatomical distance – between PRC and PHC/HC – within the representational hierarchy, for conjunction memory signals.

When collapsing across stimulus sets, I found that feature memory and conjunction memory demonstrated anatomically distinct patterns of activity, as put forth in Prediction #3. Feature memory-related activation was greatest in early ventral visual stream areas, defined either individually (V1, V2) or regionally (Early VVS), where low-level feature representations were found in the study phase. Feature memory signals decreased moving anteriorly along the VVS-MTL pathway into MTL regions. In contrast, conjunction memory-related activation was negligible in early ventral visual stream areas, defined either individually or regionally, but increased moving anteriorly into MTL regions. This finding, in line with Prediction #3, contrasts with the lack of evidence supporting Prediction #2 regarding a difference in memory signal locations for fribbles versus scenes. However, the R-H account predicts that the distance along the VVS-MTL pathway should be much greater between feature and conjunction memory than between conjunction memory signals for fribbles and scenes. Perhaps, in the context of noisy fMRI data, it is unsurprising that, of the two predictions, Prediction 3 was the one to be confirmed. Interestingly, structures that demonstrated significantly positive

conjunction memory signals (individual: PRC; regional: MTL) also contained numerically positive FCI values.

Taken together, the test phase results provide support for the notion that visual regions outside of MTL contribute to memory processes when the representational demands of a task require feature information. Additionally, foreshadowing the direct test of Prediction #4 (discussed next), the anatomical correspondence of regions involved in feature processing between the study and test phases is suggestive of support for the prediction of the R-H account that memory for feature information activates the same regions that contain representations of features. The same conclusion cannot be drawn from the current data for conjunction information (see above regarding the issue of non-significant, positive FCI values in MTL).

Finally, data from both phases of the experiment were used in a more direct test of the extent to which mnemonic signals (recorded during the second, memory test scan session) tracked perceptual representations (i.e., the properties of the neural code evoked by viewing stimuli during the first scan session) along the VVS-MTL pathway. Via a searchlight analysis of the study phase data, I first attempted to identify brain regions that demonstrated extremes of conjunction-coding (i.e., areas that reliably demonstrated an advantage for conjunction information over feature information) and feature-coding (i.e., areas that reliably demonstrated greater feature information than conjunction information) for fribbles and scenes, separately. I then analyzed the corresponding fribble/scene memory test data within the newly defined, stimulus-specific conjunction- and feature-coding regions in an analogous manner to ROI-based analyses. As put forth in Prediction #4, feature-coding regions were expected to be engaged during feature

memory and conjunction-coding regions were expected to be engaged during conjunction memory.

For both fribble and scene stimulus sets, the searchlight analysis revealed feature-coding regions that were primarily located in posterior areas of the brain, including bilaterally in LOC and fusiform and lingual gyri. In contrast, conjunction-coding regions were localized to more anterior regions of the brain. This included many cortical regions previously implicated in memory, such as anterior cingulate, lateral oribitofrontal cortex, precuneus,(Ranganath & Ritchey, 2012) and medial prefrontal cortex (Ranganath & Ritchey, 2012; Restivo, Vetere, Bontempi, & Ammassari-teule, 2009; Rugg & Vilberg, 2013).

In this analysis of the data, I was unable to find evidence of above-zero conjunction memory signals, regardless of FCI-ROI (i.e. positive FCI versus negative FCI) or stimulus set (i.e. whether ROI definition and memory score calculation used data from fribble or scene scan sessions). It may be possible that the conjunction-coding areas predicted (and found in the ROI-based memory analyses) to be the most engaged during conjunction memory (i.e., MTL) were excluded from the searchlight analysis because lower SNR levels within MTL resulted in zero or unreliable-positive FCI values, as seen in the ROI-based FCI analyses. However, feature-coding regions did demonstrate greater *feature memory* signals than conjunction-coding regions, for both fribbles and scenes. Therefore, as predicted by the R-H account, brain areas that contained feature representations during perception were also engaged during memory retrieval of that feature information.

The collection of findings described here provide some support for the R-H account, along with a number of null results that are difficult to interpret. The R-H account assumes that representations are organized along the VVS-MTL pathway such that representations are feature-based in posterior areas but transition to increasingly complex representations of conjunctions of features in more anterior areas. The present data did not allow us to fully evaluate whether the locus of the transition point from feature-coding to conjunction-coding varies for increasingly complex stimulus sets (Prediction #1) because reliable conjunction-coding areas could not be identified (i.e., none of the examined ROIs showed significantly positive FCI values). However, I acknowledge that there was reliable evidence of feature-coding areas in posterior regions for both feature sets, which did not appear to differ in location between stimulus sets (Appendix B; but, as discussed, this may have been due to the presence of similar low-level features in both sets).

The R-H theory also predicts that the locus of memory signals should be dependent on memory content, rather than confined to areas labeled as memory processing regions, i.e. MTL. There was insufficient evidence that the location of memory signals varied according to the conjunctive-complexity of stimuli in the mnemonic task (fribbles versus scenes; Prediction #2); however, there was evidence that it varied according to the complexity of to-be-retrieved information (features versus conjunctions; Prediction #3). Further, and importantly, feature memory engaged regions outside of traditional 'memory' MTL areas. Lastly, according to the R-H account, the locus of memory signals should map onto the locus of representations during perception (Prediction #4). There was insufficient evidence to support this in terms of conjunction

memory, but there was a correspondence between feature-coding areas and feature memory.

Importantly, many of the above findings are in direct conflict with existing modular theories of memory. A modular framework in which the brain is organized into independent functional components, such as ‘memory’ areas and ‘perception’ areas, is incompatible with the present findings that early and mid-ventral visual stream areas, known to be involved in perception, are also preferentially engaged during feature memory (i.e. to a greater extent than MTL regions). Consequently, further consideration should be given to the R-H theory as a plausible non-modular account of memory.

Table 1: Extreme Outliers Omitted from Statistical Analyses

Data	Analysis	ROI	Session	Subject	Level
Behavioral	Memory performance		Scenes	3	New vs. (Old + R)
					(Recomb + O) vs. New
Neural	FCI: 2x7x2 ANOVA	Individual	Fribbles	11	V1
	FCI: 2x3x2 ANOVA	Regional	Fribbles	15	Early VVS
	Memory score: 2x7x2 ANOVA	Individual	Scenes	8	PRC Conj. Memory
				23	PRC Feat. Memory
	Memory score: 7x2 ANOVA	Individual	Collapsed	8	PRC Conj. Memory
				13	PRC Feat. Memory
				18	LOC Feat. Memory
				23	PRC Feat., Memory
					PRC Conj. Memory
	Memory score: 2x3x2 ANOVA	Regional	Fribbles	23	MTL Conj. Memory
			Scenes	23	MTL Feat. Memory
	Memory score: 3x2 ANOVA	Regional	Collapsed	8	MTL Conj. Memory
				23	MTL Feat. Memory
					MTL Conj. Memory
	Memory score: 2x2 ANOVA	FCI	Scenes	8	Neg. Conj. Memory
				23	Pos. Conj. Memory

Note: Values either three times the interquartile range above the 75th quantile or below the 25th quantile were identified as extreme outliers. For repeated-measures analyses, all observations for a subject were omitted, rather than just the extreme outlier point.

Table 2: Discriminability of Mnemonic Stimulus Classes for Fribbles and Scenes

Comparison Condition	Fribble	Scene	Trial Types	Hit/Correct Rejection	False Alarm/Miss
(Familiar + R) vs. Novel	4.47	4.44	Familiar Novel	"Familiar" & "Recombination" "Novel"	"Novel" "Familiar" & "Recombination"
Familiar vs. (Novel + R)	3.28	3.59	Familiar Novel	"Familiar" "Novel" & "Recombination"	"Novel" & "Recombination" "Familiar"
Familiar vs. (Recombination + N)	2.32	2.47	Familiar Recombination	"Familiar" "Recombination" & "Novel"	"Recombination" & "Novel" "Familiar"
(Recombination + F) vs. Novel	4.37	4.22	Recombination Novel	"Recombination" & "Familiar" "Novel"	"Novel" "Recombination" & "Familiar"

Note: The *d'* statistics shown here are for each possible pairwise comparison. In each comparison, only two of the three trial types were under comparison, while any trials corresponding to the third trial type were removed from the analysis. (Trial type is indicated by non-abbreviated trial type names in the "Comparison Condition" column and listed in the "Trial Types" column). However, because there were three possible *responses* on a given trial, responses that referred to the third outstanding trial type (indicated by the initial letter of the response name – R, N or F – in the "Comparison Condition" column) were binned as a hit in some comparisons and as a false alarm in other comparisons. The exact manner in which responses referring to the outstanding trial type were treated is indicated by grouping of non-abbreviated and abbreviated trial type names via parentheses in the "Comparison Condition" column, as well as by the inclusion of two response types under the "Hit/Correct Rejection" or "False Alarm/Miss" column. For example, for the (Familiar + R) vs. Novel comparison, only Familiar and Novel trials were included in the analysis, but a participant could still respond "R" for recombination. If a participant made an "R" response during a Familiar trial, it was counted as if they had said "F" (familiar), and thus contributed to the hit rate; if a participant made an "R" response during a Novel trial, it was again counted as if they had said "F" and thus contributed to the false alarm rate. As another example, in the (Recombination + F) vs. Novel comparison, only Recombination and Novel trials were included. Here, if a participant made an "F" response during a Recombination trial, it was counted as if they had said "R" (recombination), and contributed to the hit rate, whereas an "F" response during a Novel trial counted as a false alarm.

Table 3: Ten Most Positive and Negative Voxels within Fribble FCI-ROIs

FCI-ROI	*t*-Statistic	Coordinates	Harvard-Oxford brain area
Positive	4.46	43, 36, 49	rh-precuneus
	4.45	39, 76, 29	rh-medialorbitofrontal
	4.12	36, 72, 50	lh-superiorfrontal
	3.93	36, 72, 51	lh-superiorfrontal
	3.88	35, 34, 47	lh-precuneus
	3.88	55, 62, 29	rh-parstriangularis
	3.87	40, 76, 29	rh-medialorbitofrontal
	3.78	39, 75, 29	rh-medialorbitofrontal
	3.77	39, 72, 33	rh-superiorfrontal
	3.71	54, 61, 29	rh-insula
Negative	-6.98	44, 14, 27	rh-lateraloccipital
	-6.16	19, 18, 29	lh-lateraloccipital
	-5.96	22, 20, 28	lh-lateraloccipital
	-5.82	51, 23, 23	rh-fusiform
	-5.73	22, 20, 29	lh-lateraloccipital
	-5.63	19, 19, 29	lh-lateraloccipital
	-5.63	51, 23, 24	rh-lateraloccipital
	-5.60	21, 21, 28	lh-lateraloccipital
	-5.59	52, 23, 24	rh-fusiform
	-5.55	52, 22, 24	lh-lateraloccipital

Note: Coordinates are within MNI152NLin2009cAsym standard space.
Abbreviations include *rh* for right hemisphere and *lh* for left hemisphere.

Table 4: Ten Most Positive and Negative Voxels within Scene FCI-ROIs

FCI-ROI	*t*-Statistic	Coordinates	Harvard-Oxford brain area
Positive	4.19	22, 55, 31	lh-insula
	4.10	21, 56, 31	lh-pars opercularis
	4.01	22, 54, 31	lh-insula
	3.95	38, 70, 36	lh-rostralanteriorcingulate
	3.92	22, 56, 31	lh-insula
	3.91	39, 70, 39	rh-superiorfrontal
	3.90	21, 55, 31	lh-insula
	3.87	47, 28, 59	rh-superiorparietal
	3.85	51, 72, 27	rh-lateralorbitofrontal
	3.83	39, 70, 38	rh-superiorfrontal
Negative	-8.15	25, 16, 37	lh-inferiorparietal
	-7.41	25, 17, 37	lh-inferiorparietal
	-7.17	25, 17, 36	lh-inferiorparietal
	-6.80	25, 16, 36	lh-inferiorparietal
	-6.78	30, 22, 29	lh-lingual
	-6.66	26, 16, 36	lh-lateraloccipital
	-6.56	24, 16, 37	lh-lateraloccipital
	-6.51	25, 15, 37	lh-inferiorparietal
	-6.36	28, 22, 30	lh-fusiform
	-6.34	26, 16, 37	lh-lateraloccipital

Note: Coordinates are within MNI152NLin2009cAsym standard space.
Abbreviations include *rh* for right hemisphere and *lh* for left hemisphere.

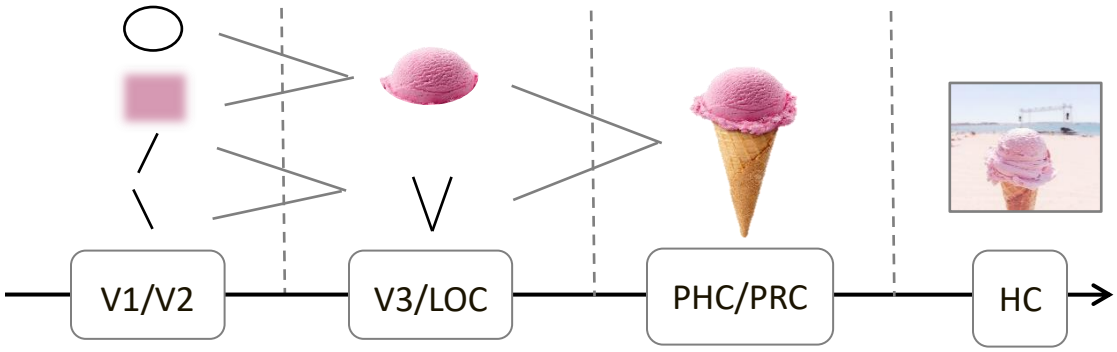

Figure 1: Illustration of Representational Organization. The R-H account assumes that the complexity of a representation is determined by the dimensionality of the representation. Individual features are represented in posterior areas of a ventral-visual-stream-to-MTL pathway (e.g. early visual cortex: V1, V2). Conjunctions of those features are represented in more anterior regions of the pathway (e.g. V3, LOC) and continue to increase in dimensionality moving anteriorly (e.g., PHC, PRC). The hierarchy is assumed to culminate in HC, which represents the conjunction of an item within its spatial and/or temporal context.

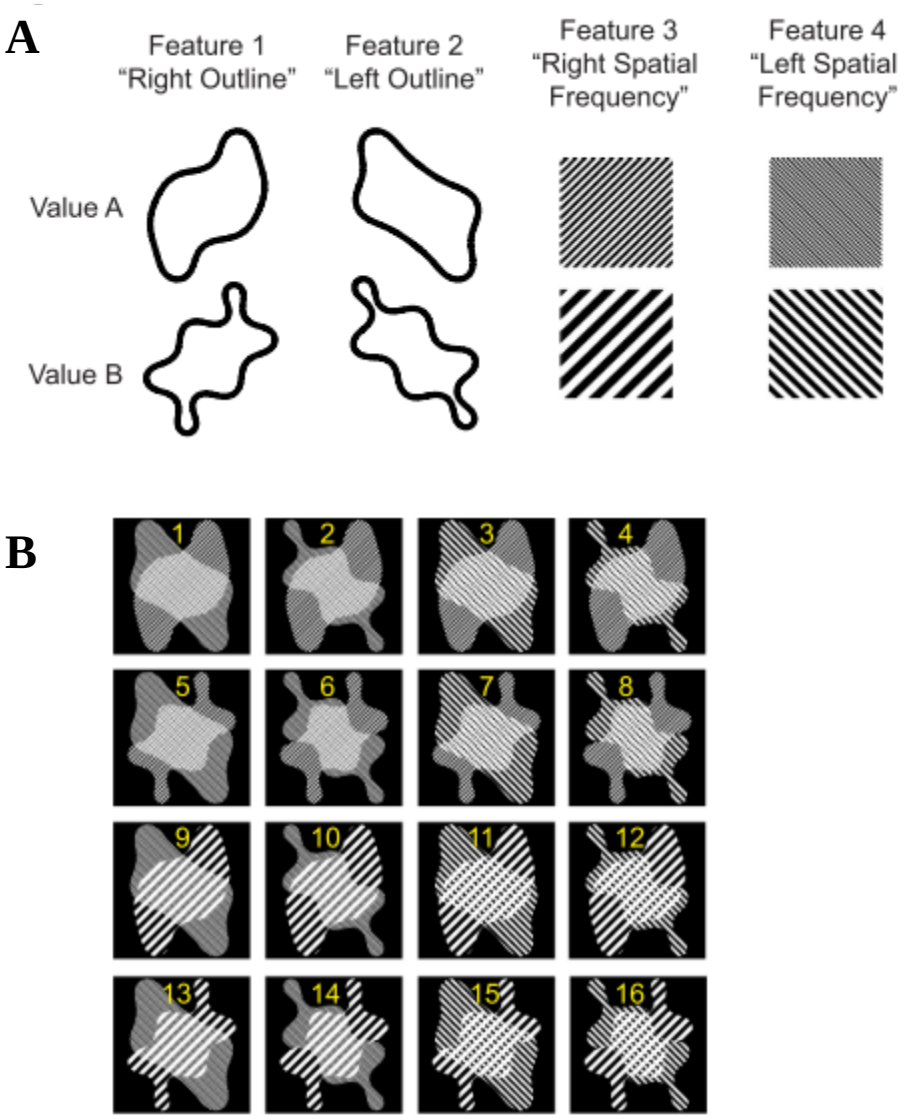

Figure 2: Simple Object Stimuli from Cowell et al. (2017), adapted with permission. *A*: Stimuli were constructed by conjoing four binary (Values A and B) features (Right Outline, Left Outline, Right Spatial Frequncy and Left Spatial Frequncy); *B*: All possible combinations of the four binary features created sixteen unique conjunctive simple object stimuli.

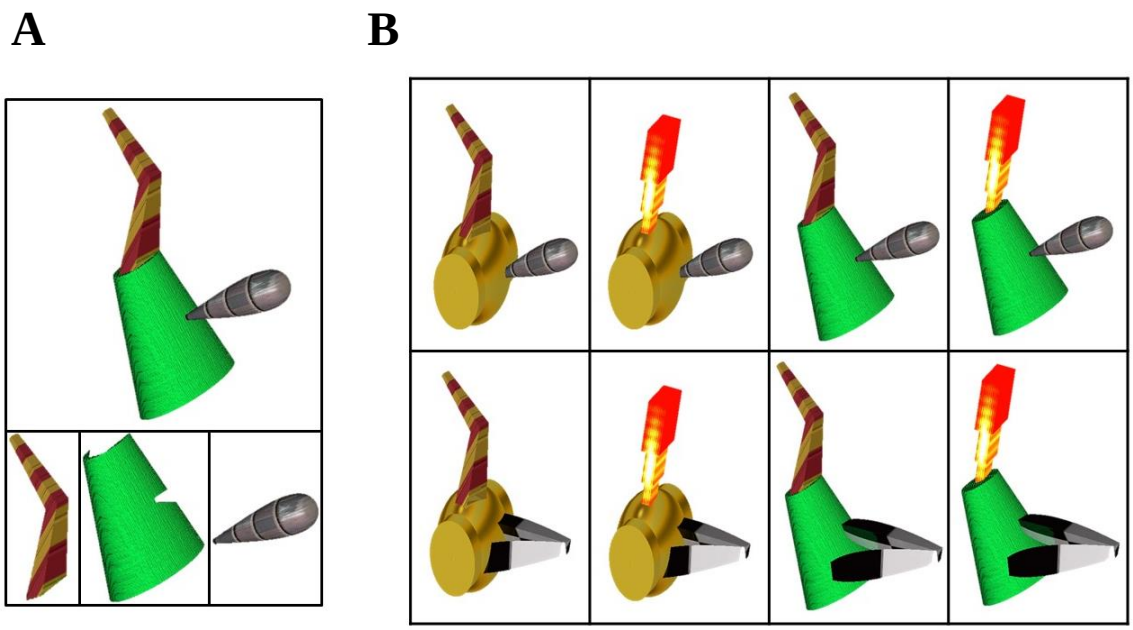

Figure 3: Fribble Stimulus Set Examples. *A*: a conjunctive fribble (top) and "tail", "body" and "head" features (bottom, left to right); *B*: A family containing eight unique conjunctive fribbles, constructed from three binary features.

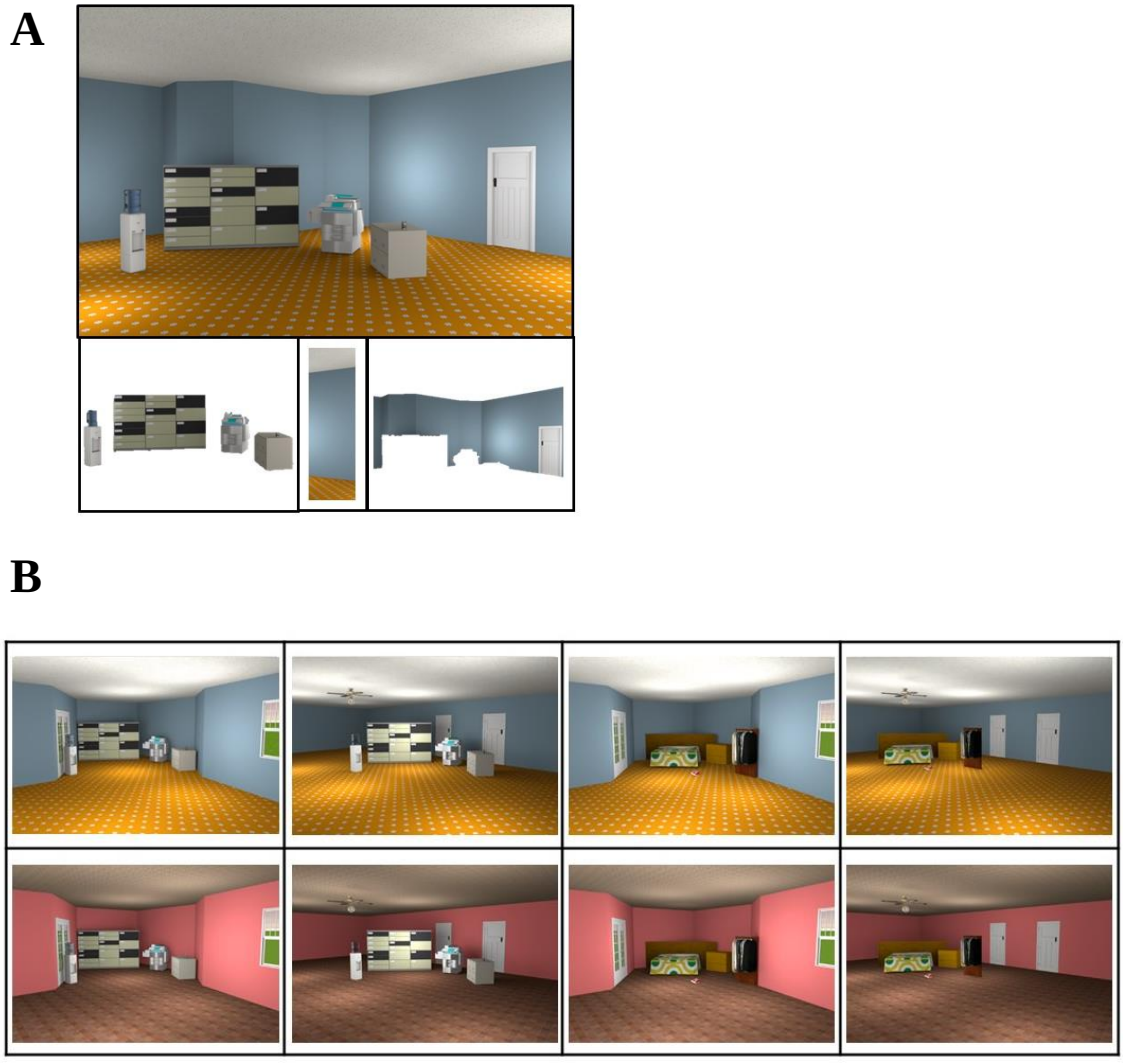

Figure 4: Scene Stimulus Set Examples. *A*: a conjunctive scene (top) and room furniture, color and shape features (bottom, left to right); *B*: A family containing eight unique conjunctive scenes composed using three binary room features.

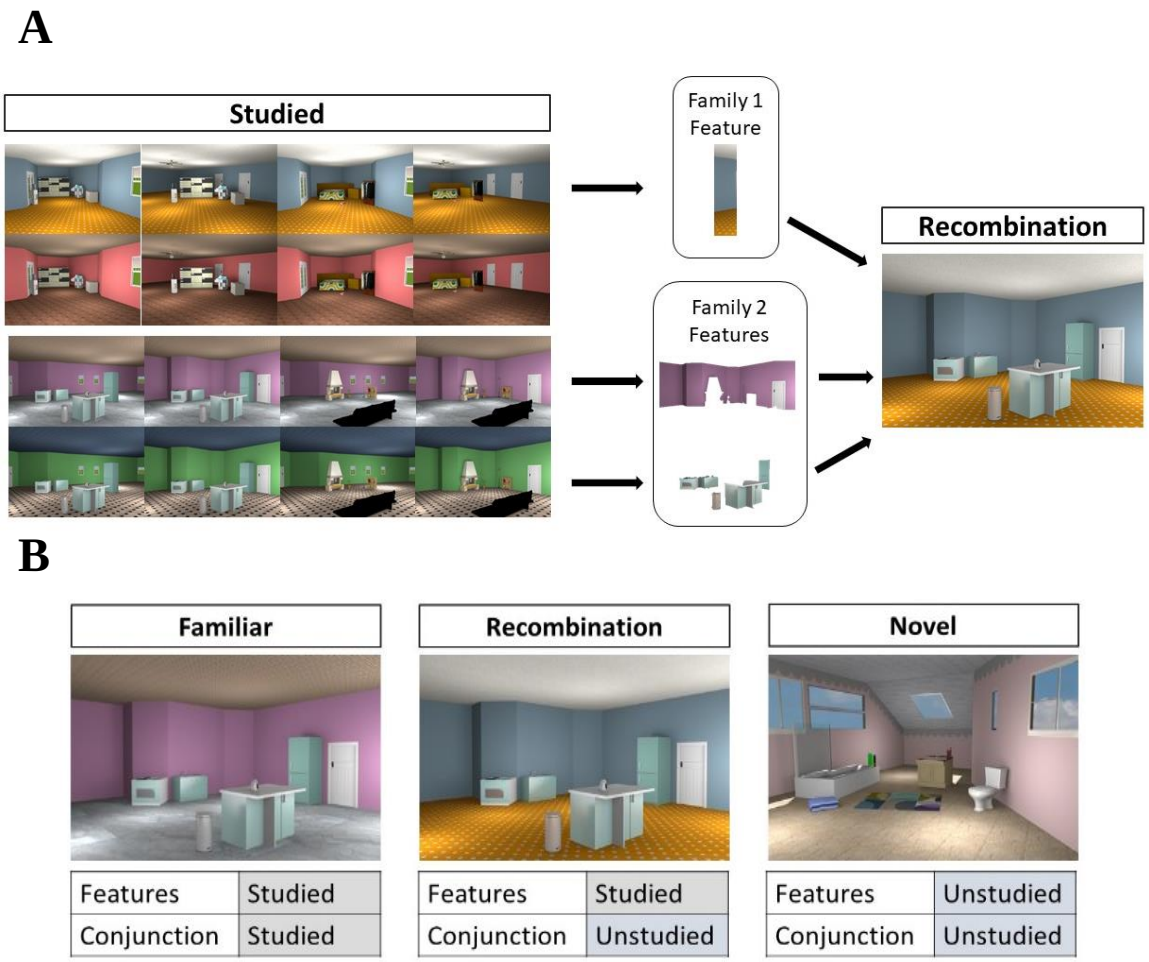

Figure 5: Scene Stimulus Set Recombination Examples. *A*: counterbalanced across participants, two families from the scene stimulus set were designated to be studied (i.e., presented in the first scan session). In this example, a Recombination stimulus is created by combining the color feature from the first family with the room shape and furniture features from the second family. All potential '1 + 2' feature combinations within a given family pairing yielded 48 Recombination stimuli; *B*: the three mnemonic stimulus classes differed on the basis of whether features and the conjunction of features were studied prior to the memory test.

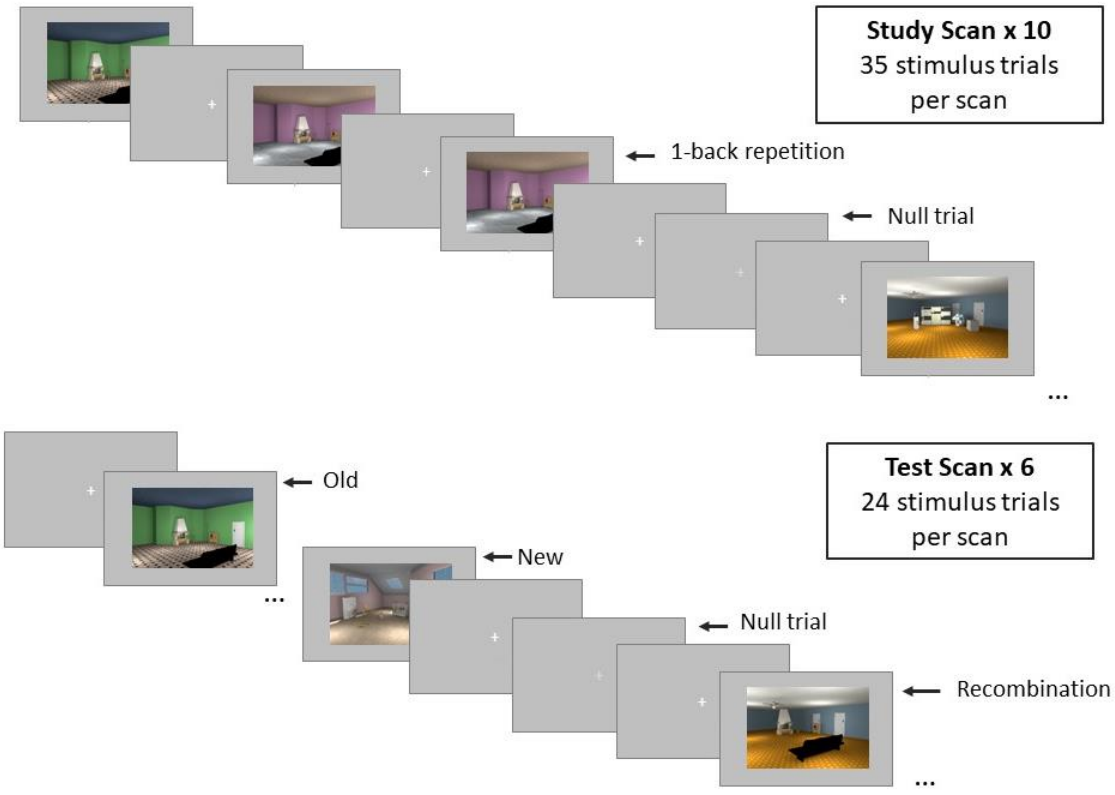

Figure 6: Experimental Design. During a study scan, participants indicated if the current image was identical to the image immediately before (i.e., 1-back repetition task). During a test scan, participants distinguished between Familiar, Novel, and Recombination stimuli. Both study and test scans featured null trials where participants indicated if a fixation cross dimmed. Participants completed ten study scans and then exited the scanner for a self-paced break. When participant re-entered the scanner, they completed six test scans. Scene stimuli are shown here, but the experimental protocol was identical for the fribble scan sessions, which were completed on a separate day.

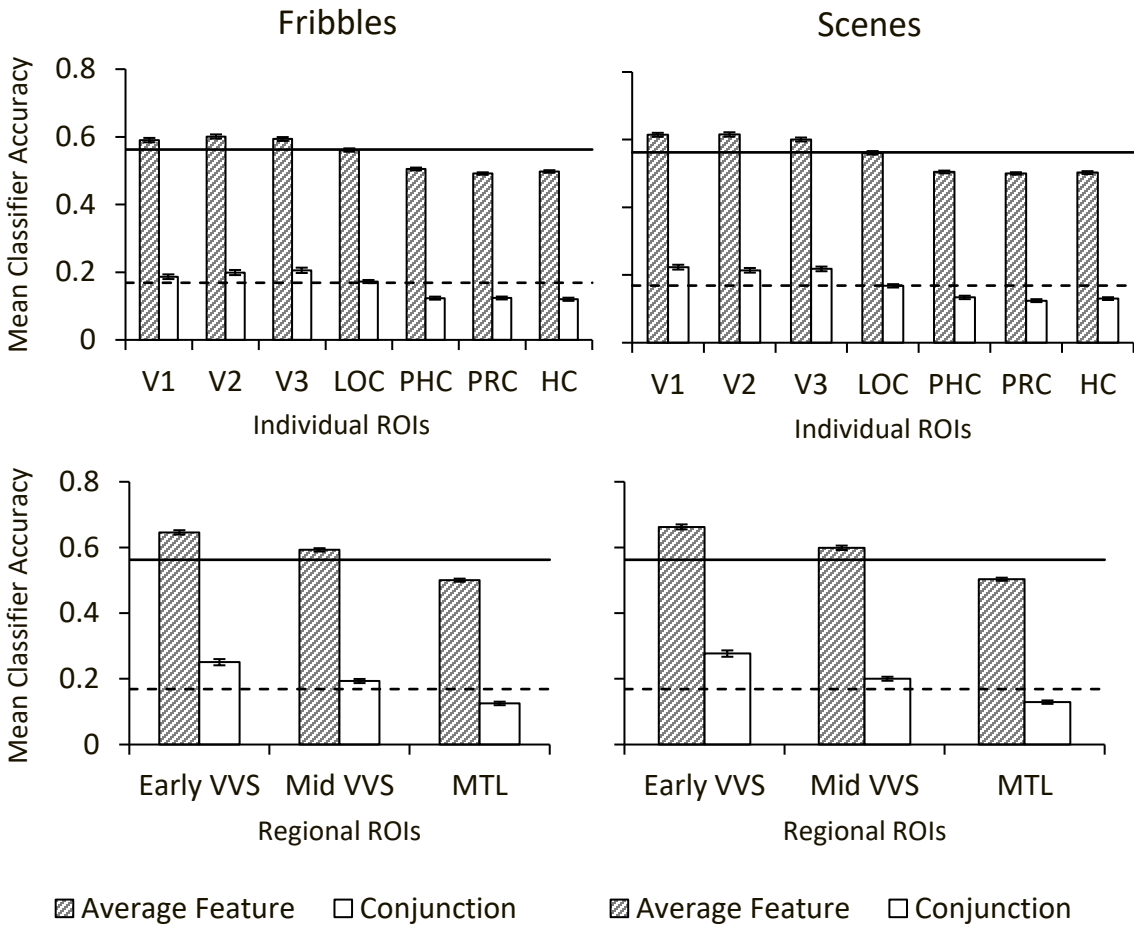

Figure 7: Study Phase Classifier Accuracies by Stimulus Set and ROI Selection. Classifier accuracies were averaged over the two studied family sets from a stimulus set, for each subject. The average of the three two-way feature-classifiers is displayed above. Accuracy levels indicating classifier performance above chance were determined with a binomial test, uncorrected for multiple comparisons. This accuracy level was 0.5625 for feature-classifiers (solid line) and 0.1628 for the conjunction-classifier (dashed lined). Error bars are within-subject SEM. Both feature- and conjunction-classifier accuracies were not significantly greater than chance performance for MTL structures, regardless of stimulus set (fribbles [left] versus scenes [right]) or how ROIs were defined (individually [top] versus regionally [bottom]).

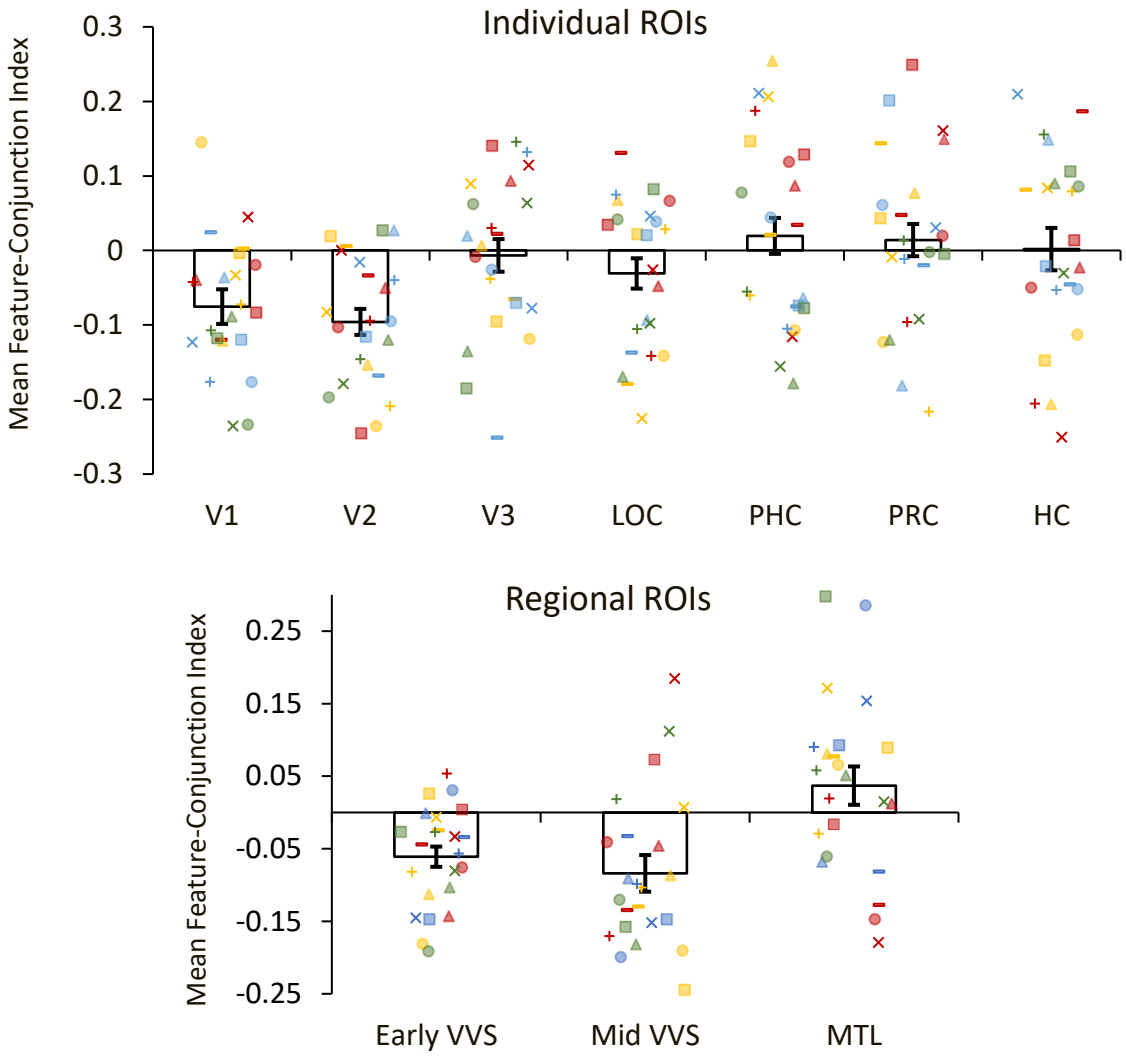

Figure 8: Study Phase Feature-Conjunction Indexes (FCIs) by ROI Selection. FCIs were derived by taking the natural log of the ratio of conjunction classifier accuracy (i.e., *empirically observed* conjunction accuracy) to the product of three feature classifier accuracies (i.e., *predicted* conjunction accuracy; see Methods for further detail). A negative FCI reflects feature-coding, while a positive FCI reflects conjunction-coding. FCIs were first averaged across the two studied family sets from a given stimulus set, and then across the two stimulus sets for each subject. White bars show group means; plotted points show individual subjects, where each unique color-marker combination corresponds to the same individual subject across ROIs. Error bars are within-subject SEM. Regardless of whether ROIs were defined individually (top) or regionally (bottom), feature-coding (i.e., negative FCIs) appeared to transition to a different form of coding — either a 'hybrid' combination of feature- and conjunction-coding (i.e., zero FCIs) or conjunction-coding (i.e., positive FCIs) — when moving anteriorly along the VVS-MTL pathway. MTL FCI values should be interpreted with caution; classifier accuracies were not above chance and thus zero FCIs could indicate 'hybrid' coding or an absence of feature- and conjunction-knowledge altogether.

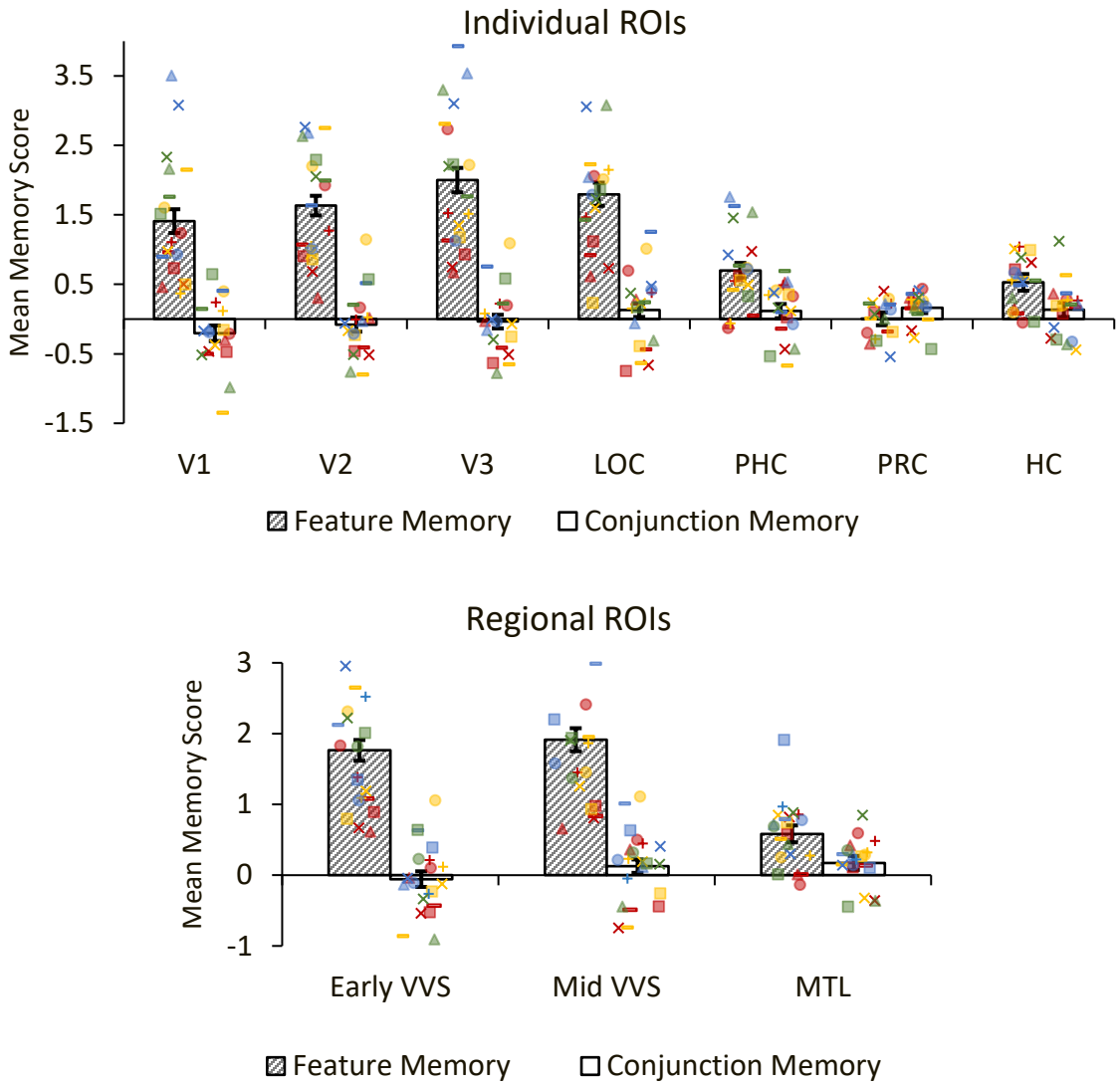

Figure 9: Test Phase Memory Scores by ROI Selection. Memory scores were derived by calculating the effect size, as measured by Cohen's D, for the contrast of Novel and Recombination trials (i.e., Feature Memory) and for the contrast of Recombination and Familiar trials (i.e., Conjunction Memory). Memory scores were averaged across the two stimulus sets, for each subject. Stripped and solid white bars show group means; plotted points show individual subjects, where each unique color-marker combination corresponds to the same individual subject across ROIs. Error bars are within-subject SEM. Regardless of whether ROIs were defined individually (top) or regionally (bottom), signals for feature memory were greatest in posterior areas along a VVS-MTL pathway. In contrast, signals for conjunction memory were greatest in MTL areas.

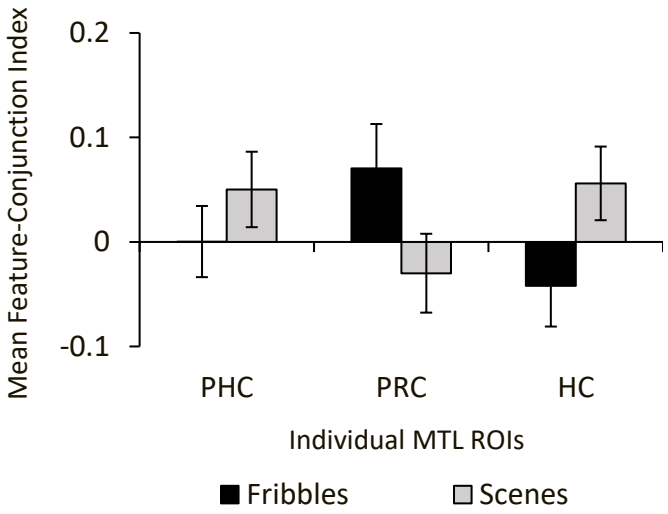

Figure 10: Study Phase Feature-Conjunction Indexes (FCIs) by Stimulus Set for Individual MTL ROIs Only. FCIs did not vary between fribble and scene stimulus sets when considering all seven individual ROIs (see Section 2.3.1). However, when analyzing only a subset of individual ROIs that fall within MTL, there was an interaction between stimulus set and ROI, such that PRC contained the most positive FCIs for fribbles and PHC and HC contained the most positive FCIs for scenes. This demonstrates that there may in fact be differences in the locus of conjunction-coding between different types of stimuli and supports the methodological decision to define FCI-ROIs separately for each stimulus set in the searchlight analysis.

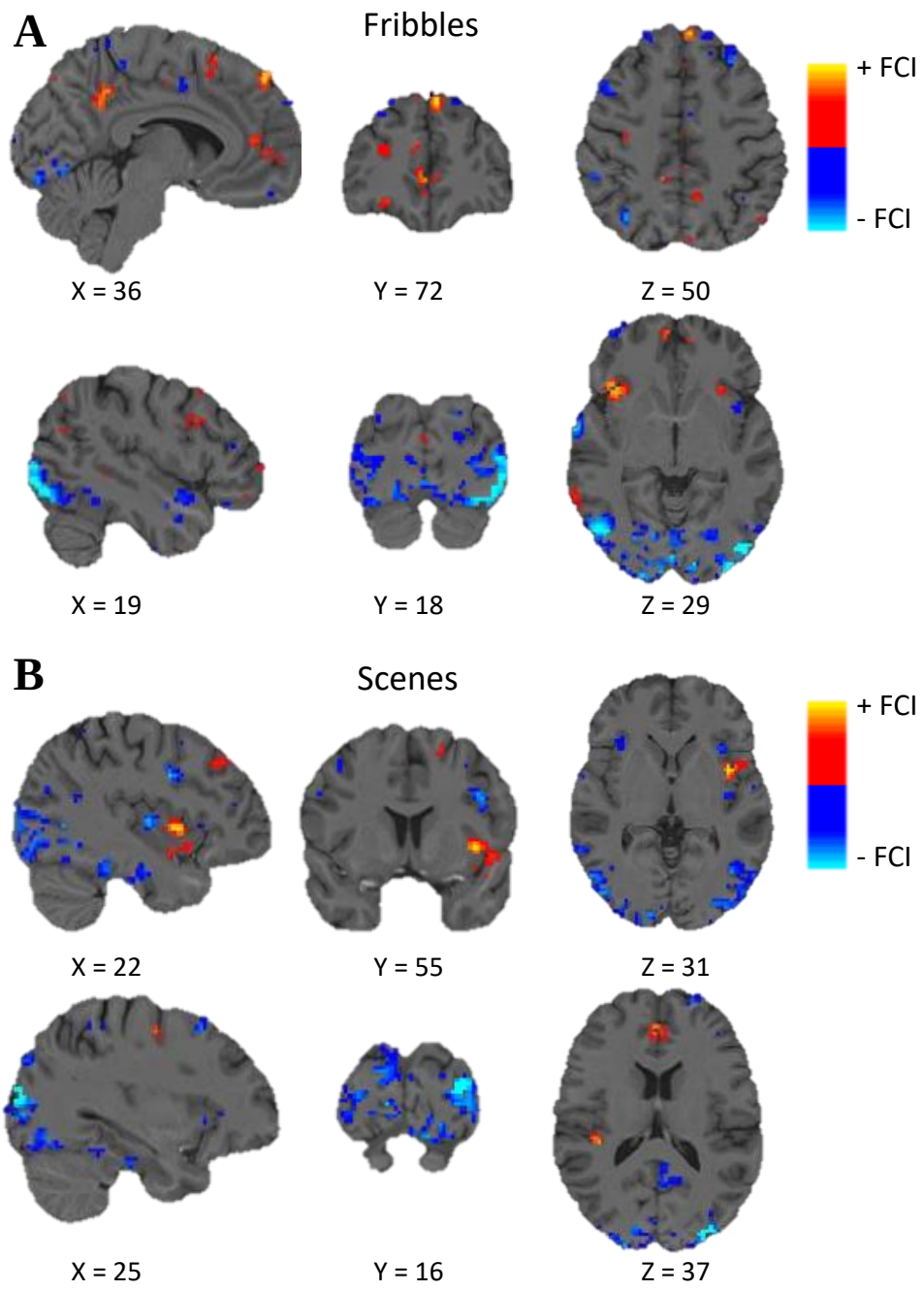

Figure 11: FCI-ROIs Defined via Searchlight Analysis of Study Phase Data. For each stimulus set and subject separately, FCI was recorded at each center voxel of a spherical ROI swept throughout the brain. Voxels that demonstrated FCIs significantly less than or greater than zero via a group-level *t*-test were grouped into negative and positive FCI-ROIs, respectively. Negative FCI-ROIs (blue) indicate regions that demonstrated statistically reliable extremes of feature-coding and positive FCI-ROIs (red) indicate regions that demonstrated statistically reliable extremes of conjunction-coding. For both fribbles (*A*) and scenes (*B*), top and bottom rows show the same FCI-ROIs, but from different views to highlight positive and negative areas.

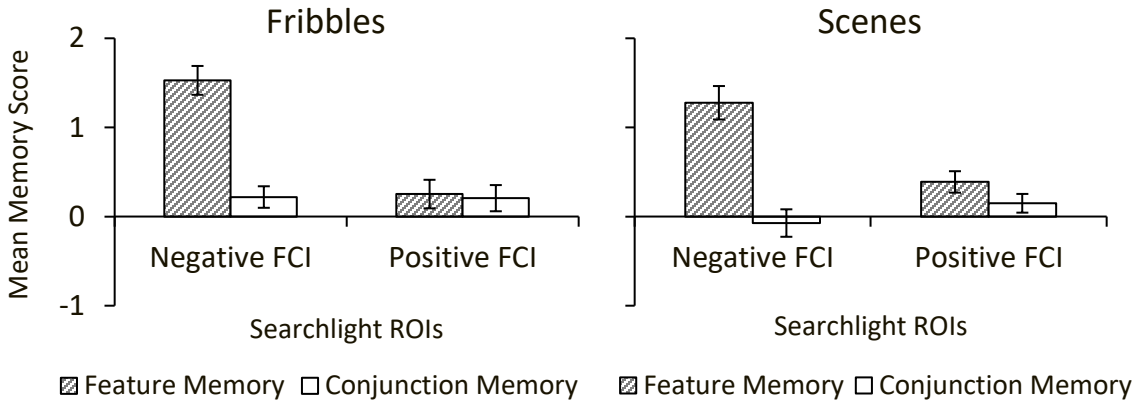

Figure 12: Test Phase Memory Scores for FCI-defined ROIs. For both fribble (left) and scene (right) stimulus sets, negative FCI-ROIs included brain areas that contain more information about individual features than the conjunction of those features (i.e. feature-coding), based on study phase data collected while participants viewed the stimuli. In contrast, positive FCI-ROIs included brain areas that contain more information about the conjunction of features than about those features separately (i.e. conjunction-coding). Memory scores for stimulus-specific, FCI-defined ROIs were derived from corresponding fribble/scene memory test phase data in an identical manner to the memory scores for *a priori* individual and regional ROIs. Feature memory was measured by the effect size (Cohen's D) of the contrast between Novel and Recombination trials; conjunction memory was measured by the effect size of the contrast between Recombination and Familiar trials. Error bars are within-subject SEM. For both fribble and scene stimulus sets, signals for feature memory were greater in feature-coding ROIs than in conjunction-coding ROIs.

APPENDIX A

IMAGING DATA PREPROCESSING

The fMRI results included in this dissertation were derived from preprocessing performed using fMRIPrep 1.5.2 (Esteban et al., 2019, 2018; RRID:SCR_016216), which is based on Nipype 1.3.1 (Esteban et al., 2018; Gorgolewski et al., 2011; RRID:SCR_002502). The following description of the preprocessing procedure is based on the boilerplate automatically generated by fMRIPrep (CC0 license), though the text has been edited for the purpose of clarity.

Anatomical data preprocessing

First, each of the two T1-weighted (T1w) images (one image obtained for each of the two stimulus set scan sessions, collected on separate days) were corrected for intensity non-uniformity (INU; an imaging artifact when, as a result of acquisition techniques or patient movement, voxels belonging to the same tissue type demonstrate intensity variations across images). INU correction was completed using N4BiasFieldCorrection (Tustison et al., 2010), distributed with ANTs 2.2.0 (Avants, Epstein, Grossman, & Gee, 2008, RRID:SCR_004757). The T1w images were then skull-stripped with a Nipype implementation of the antsBrainExtraction.sh workflow (from ANTs), using OASIS30ANTs as the target template. Brain tissue segmentation of cerebrospinal fluid (CSF), white-matter (WM) and gray-matter (GM) was performed on the brain-extracted T1w images using FAST (FSL 5.0.9, RRID:SCR_002823, Zhang, Brady, & Smith, 2001).

Next, a single T1w-reference map was computed after registration of the two T1w images using mri_robust_template (FreeSurfer 6.0.1, Reuter, Rosas, & Fischl, 2010). The

registration was unbiased, such that the resulting template was equidistant from both T1w source images. This preprocessed T1w reference defined the T1w space and was used throughout the preprocessing workflow (i.e., all reconstructed surfaces and functional datasets were registered to this averaged T1w reference, and not to either of the T1w source images).

Then brain surfaces were reconstructed using recon-all (FreeSurfer 6.0.1, RRID:SCR_001847, Dale, Fischl, & Sereno, 1999) and the brain mask, derived via ANTs during the earlier skull-stripping of the T1w images, was refined with a custom variation of the method to reconcile ANTs-derived and FreeSurfer-derived segmentations of the cortical gray-matter of Mindboggle (RRID:SCR_002438, Klein et al., 2017). This refinement of the brain mask addresses common inaccuracies in the ANTS-derived brain mask, such as small amounts of MR signal from outside of the brain.

In a final step, spatial normalization to the ICBM 152 Nonlinear Asymmetrical template version 2009c [Fonov et al. (2009), RRID:SCR_008796; TemplateFlow ID: MNI152NLin2009cAsym] was performed through nonlinear registration with the antsRegistration tool (ANTs 2.2.0), using brain-extracted versions of both the T1w reference and the standard space template.

Functional data preprocessing

For each of the 34 BOLD scans gathered for a given subject (i.e., 10 study scans, 6 test scans, and 1 functional localizer, collected for each of the two stimulus sets, on separate days), the following preprocessing was performed. First, a BOLD reference image and its skull-stripped version were generated using a custom methodology of fMRIPrep. Using this BOLD reference, head-motion parameters (transformation

matrices, and six corresponding rotation and translation parameters) were estimated using mcflirt (FSL 5.0.9, Jenkinson et al. 2002). The six rotation and translation parameters were later included as motion nuisance regressors in GLM estimates of both the study and test data.

The BOLD reference was also used to correct for susceptibility distortions (an imaging artifact that results in points of extreme intensity, either very dark or very bright, in an image because of differences in the magnetic field). Specifically, using a custom workflow of fMRIPrep derived from D. Greve's epidewarp.fsl script and further improvements of HCP Pipelines (Glasser et al., 2013), a deformation field was estimated based on a field map that was co-registered to the BOLD reference. Using this estimated susceptibility distortion, an unwarped BOLD reference was calculated for a more accurate co-registration with the anatomical (T1w) reference. The unwarped BOLD reference was then co-registered to the T1w reference using bbregister (FreeSurfer), which implements boundary-based registration (Greve & Fischl, 2009). Co-registration was configured with six degrees of freedom to account for remaining distortions in the new BOLD reference.

Next, the BOLD time-series were resampled to two volumetric spaces: subject native space and MNI152NLin2009cAsym standard space. Note that all resamplings were performed with a single interpolation step by concatenating all the pertinent transformations (i.e. head-motion transform matrices, susceptibility distortion correction, and co-registrations to anatomical and output spaces) in order to minimize information lost. Volumetric (gridded) resamplings were performed using antsApplyTransforms (ANTs), configured with Lanczos interpolation to minimize the smoothing effects of

other kernels (Lanczos, 1964). The BOLD time-series resampled in the MNI152NLin2009cAsym standard space was only used for the searchlight analysis, which required data from multiple subjects to be transformed into a common space for definition of group-level FCI-ROIs. The BOLD time-series resampled in native space was used for all other analyses (i.e., individual and regional ROI-based analyses of FCI values and memory scores).

Following volumetric resampling, the BOLD time-series were resampled to two surface spaces: subject native space (fsnative) and the fsaverage template space. Surface (non-gridded) resamplings were performed using mri_vol2surf (FreeSurfer). The transformation matrices created during the surface resamplings were later used to apply the probabilistic ROI atlases to each subject.

Additionally, several other parameters were automatically extracted based on the preprocessed BOLD time-series resampled in volumetric native space. This included framewise displacement (FD), DVARS and three region-wise global signals, as well as a set of physiological regressors to allow for component-based noise correction (CompCor, Behzadi et al. 2007). However, because these parameters were ultimately not used as nuisance regressors in the GLM estimation of the study and test data, the exact details of how these parameters were calculated will not be expanded on here.

Many internal operations of fMRIPrep use Nilearn 0.5.2 (Abraham, Pedregosa, Eickenberg, & Gervais, 2014, RRID:SCR_001362), mostly within the functional processing workflow. For more details of the pipeline, see the section corresponding to workflows in fMRIPrep's documentation: https://fmriprep.org/en/1.5.2/workflows.html.

APPENDIX B

STIMULUS-SPECIFIC FEATURE-CONJUNCTION INDEXES

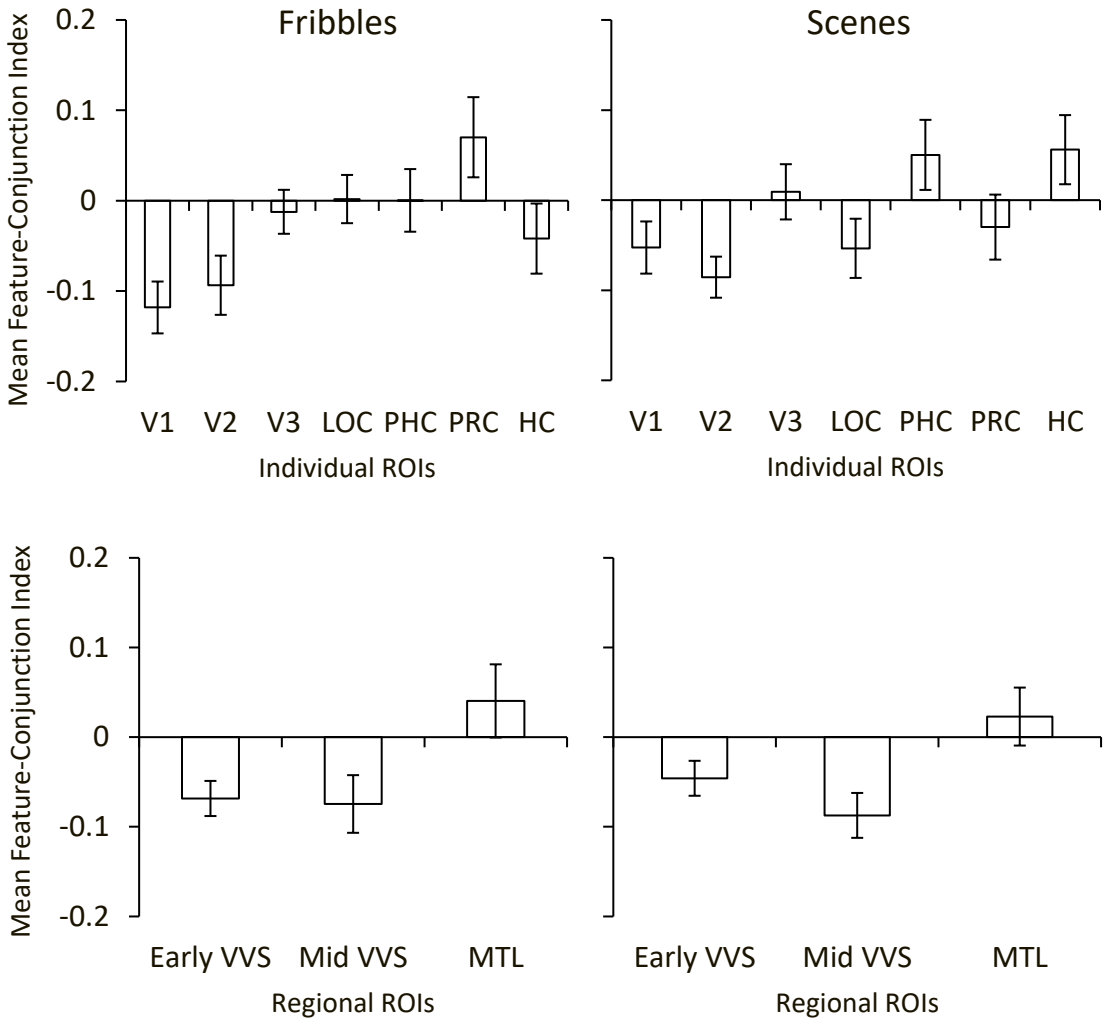

Figure B1: Study Phase Feature-Conjunction Indexes (FCIs) by ROI Selection and Stimulus Set Type. For both individual (top) and regional (bottom) ROI-based analyses, FCIs were derived by taking the natural log of the ratio of conjunction classifier accuracy (i.e., *empirically observed* conjunction accuracy) to the product of three feature classifier accuracies (i.e., *predicted* conjunction accuracy; see Methods for further detail). A negative FCI reflects feature-coding, while a positive FCI reflects conjunction-coding. FCIs were averaged across the two studied family sets from a given stimulus set for each subject. Error bars are within-subject SEM. There was not sufficient evidence that FCI values differed between fribble (left) and scene (right) stimulus sets when all ROIs were included in the analysis (though stimulus set-related differences existed in a subset of individual MTL regions). Consequently, FCI values were averaged across stimulus set for all further analyses.

APPENDIX C

STIMULUS-SPECIFIC MEMORY SCORES

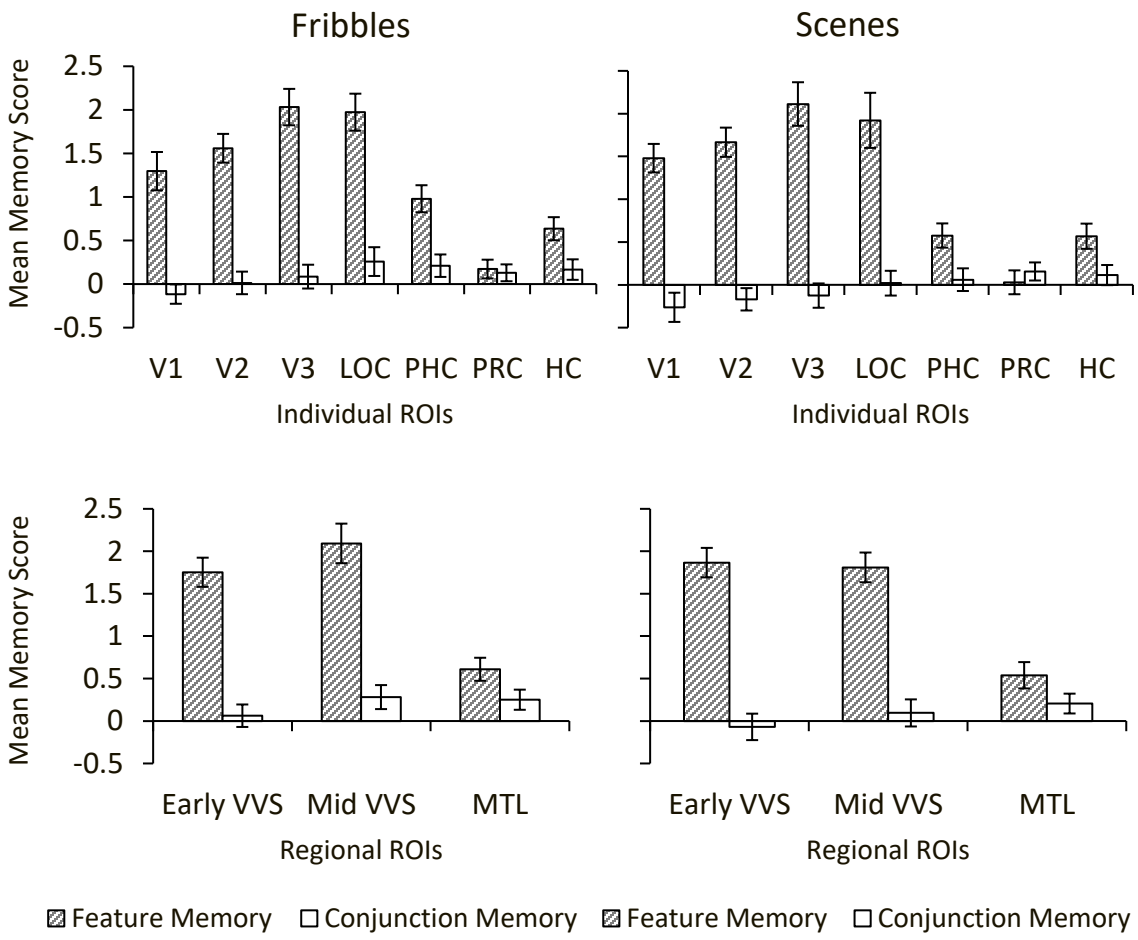

Figure C1: Test Phase Memory Scores by ROI Selection and Stimulus Set Type. For both individual (top) and regional (bottom) ROI-based analyses, memory scores were derived by calculating the effect size, as measured by Cohen's D, for the contrast of Novel and Recombination trials (i.e., Feature Memory) and for the contrast of Recombination and Familiar trials (i.e., Conjunction Memory). Error bars are within-subject SEM. There was insufficient evidence of stimulus set-related differences in memory scores to justify treating the stimulus sets separately in this ROI-based analysis of memory. Consequently, memory scores were averaged across fribble (left) and scene (right) stimulus sets for all further ROI-based analyses.

REFERENCES

Abraham, A., Pedregosa, F., Eickenberg, M., & Gervais, P. (2014). Machine learning for neuroimaging with scikit-learn. *Frontiers in Neuroinformatics*, *8*(14), 1–10. https://doi.org/10.3389/fninf.2014.00014

Aggleton, J. P., & Brown, M. W. (1999). Episodic memory, amnesia, and the hippocampal-anterior thalamic axis. *Behavioral and Brain Sciences*, *22*, 425–489.

Avants, B. B., Epstein, C. L., Grossman, M., & Gee, J. C. (2008). Symmetric diffeomorphic image registration with cross-correlation: Evaluating automated labeling of elderly and neurodegenerative brain. *Medical Image Analysis*, *12*(1), 26–41. https://doi.org/10.1016/j.media.2007.06.004

Barense, M. D., Bussey, T. J., Lee, A. C. H., Rogers, T. T., Davies, R. R., Saksida, L. M., … Graham, K. S. (2005). Functional Specialization in the Human Medial Temporal Lobe. *The Journal of Neuroscience*, *25*(44), 10239–10246. https://doi.org/10.1523/JNEUROSCI.2704-05.2005

Barense, M. D., Henson, R. N. a, Lee, A. C. H., & Graham, K. S. (2010). Medial temporal lobe activity during complex discrimination of faces, objects, and scenes: Effects of viewpoint. *Hippocampus*, *20*(3), 389–401. https://doi.org/10.1002/hipo.20641

Barry, T. J., Griffith, J. W., De Rossi, S., & Hermans, D. (2014). Meet the fribbles: Novel stimuli for use within behavioural research. *Frontiers in Psychology*, *5*, 1–8. https://doi.org/10.3389/fpsyg.2014.00103

Bartko, S. J., Cowell, R. A., Winters, B. D., Bussey, T. J., & Saksida, L. M. (2010). Heightened susceptibility to interference in an animal model of amnesia: Impairment in encoding, storage, retrieval - or all three? *Neuropsychologia*, *48*, 2987–2997. https://doi.org/10.1016/j.neuropsychologia.2010.06.007

Bartko, S. J., Winters, B. D., Cowell, R. A., Saksida, L. M., & Bussey, T. J. (2007a). Perceptual functions of perirhinal cortex in rats: zero-delay object recognition and simultaneous oddity discriminations. *The Journal of Neuroscience*, *27*(10), 2548–2559. https://doi.org/10.1523/JNEUROSCI.5171-06.2007

Bartko, S. J., Winters, B. D., Cowell, R. A., Saksida, L. M., & Bussey, T. J. (2007b). Perirhinal cortex resolves feature ambiguity in configural object recognition and perceptual oddity tasks. *Learning & Memory*, *14*, 821–832. https://doi.org/10.1101/lm.749207

Behzadi, Y., Restom, K., Liau, J., & Liu, T. T. (2007). A component based noise correction method (CompCor) for BOLD and perfusion based fMRI. *Human Brain Mapping Journal*, *37*(1), 90–101. https://doi.org/10.1016/j.neuroimage.2007.04.042

Blake, L., Jarvis, C. D., & Mishkin, M. (1977). Pattern discrimination thresholds after

partial inferior temporal of lateral striate lesions in monkeys. *Brain Research*, *120*, 209–220.

Brown, M. W., & Aggleton, J. P. (2001). Recognition memory: What are the roles of the perirhinal cortex and hippocampus? *Nature Reviews Neuroscience*, *2*(1), 51–61. https://doi.org/10.1038/35049064

Buckley, M. J., Booth, M. C., Rolls, E. T., & Gaffan, D. (2001). Selective perceptual impairments after perirhinal cortex ablation. *J Neurosci*, *21*(24), 9824–9836. Retrieved from http://eutils.ncbi.nlm.nih.gov/entrez/eutils/elink.fcgi?dbfrom=pubmed&id=11739590&retmode=ref&cmd=prlinks

Bussey, T. J., & Saksida, L. M. (2002). The organization of visual object representations: A connectionist model of effects of lesions in perirhinal cortex. *The European Journal of Neuroscience*, *15*, 355–364. https://doi.org/10.1046/j.0953-816x.2001.01850.x

Bussey, T. J., Saksida, L. M., & Murray, E. A. (2002). Perirhinal cortex resolves feature ambiguity in complex visual discriminations. *European Journal of Neuroscience*, *15*, 365–374. https://doi.org/10.1046/j.0953-816x.2001.01851.x

Bussey, T. J., Saksida, L. M., & Murray, E. A. (2003). Impairments in visual discrimination after perirhinal cortex lesions: Testing "declarative" vs. "perceptual-mnemonic" views of perirhinal cortex function. *European Journal of Neuroscience*, *17*(3), 649–660. https://doi.org/10.1046/j.1460-9568.2003.02475.x

Clarke, A., & Tyler, L. K. (2014). Object-specific semantic coding in human perirhinal cortex. *Journal of Neuroscience*, *34*(14), 4766–4775. https://doi.org/10.1523/JNEUROSCI.2828-13.2014

Cooke, S. F., Komorowski, R. W., Kaplan, E. S., Gavornik, Jeffrey, P., & Bear, M. F. (2015). Visual recognition memory, manifest as long-term habituation, requires synaptic plasticity in V1. *Nature Ne*, *18*(2), 262–271. https://doi.org/10.1038/nn.3920

Cosmides, L., & Tooby, J. (1994). Beyond intuition and instinct blindness: toward an evolutionarily rigorous cognitive science. *Cognition*, *50*, 41–77. https://doi.org/10.1016/0010-0277(94)90020-5

Cowell, R. A., Barense, M. D., & Sadil, P. S. (2019). A Roadmap for Understanding Memory: Decomposing Cognitive Processes into Operations and Representations. *ENeuro*, *6*(4).

Cowell, R. A., Bussey, T. J., & Saksida, L. M. (2006). Why does brain damage impair memory? A connectionist model of object recognition memory in perirhinal cortex. *The Journal of Neuroscience*, *26*(47), 12186–12197. https://doi.org/10.1523/JNEUROSCI.2818-06.2006

Cowell, R. A., Bussey, T. J., & Saksida, L. M. (2010). Components of recognition memory: Dissociable cognitive processes or just differences in representational complexity? *Hippocampus*, *20*, 1245–1262. https://doi.org/10.1002/hipo.20865

Cowell, R. A., Leger, K., & Serences, J. T. (2017). Feature-coding transitions to conjunction-coding with progression through human visual cortex. *Journal of Neurophysiology*, jn.00503.2017. https://doi.org/10.1152/jn.00503.2017

Cowey, A., & Gross, C. G. (1970). Effects of foveal prestriate and inferotemporal lesions on visual discrimination by rhesus monkeys. *Experimental Brain Research*, *11*, 128–144.

Dale, A. M., Fischl, B., & Sereno, M. I. (1999). Cortical Surface-Based Analysis: I. Segmentation and Surface Reconstruction. *NeuroImage*, *9*(2), 179–194.

Davachi, L. (2006). Item, context and relational episodic encoding in humans. *Current Opinion in Neurobiology*, *16*(6), 693–700. https://doi.org/10.1016/j.conb.2006.10.012

Davachi, L., Mitchell, J. P., & Wagner, A. D. (2003). Multiple routes to memory: Distinct medial temporal lobe processes build item and source memories. *Proceedings of the National Academy of Sciences*, *100*(4), 2157–2162. https://doi.org/10.1073/pnas.0337195100

Delhaye, E., Bahri, M. A., Salmon, E., & Bastin, C. (2019). Impaired perceptual integration and memory for unitized representations are associated with perirhinal cortex atrophy in Alzheimer's disease. *Neurobiology of Aging*, *73*, 135–144. https://doi.org/10.1016/j.neurobiolaging.2018.09.021

Desimone, R., & Ungerleider, L. G. (1989). *Handbook of Neuropsychology*. (F. Boller & J. Grafman, Eds.). Amsterdam: Elsevier.

Diana, R. A., Yonelinas, A. P., & Ranganath, C. (2007). Imaging recollection and familiarity in the medial temporal lobe: a three-component model. *Trends in Cognitive Sciences*, *11*(9), 379–386. https://doi.org/10.1016/j.tics.2007.08.001

Eacott, M. J., Gaffan, D., & Murray, E. A. (1994). Preserved recognition memory for small sets, and impaired stimulus identification for large sets, following rhinal cortex ablations in monkeys. *Eur J Neurosci*, *6*(9), 1466–1478. https://doi.org/10.1111/j.1460-9568.1994.tb01008.x

Eichenbaum, H., Yonelinas, A. P., & Ranganath, C. (2007). The medial temporal lobe and recognition memory. *Annual Review of Neuroscience*, *30*(1), 123–152. https://doi.org/10.1146/annurev.neuro.30.051606.094328

Erez, J., Cusack, R., Kendall, W., & Barense, M. D. (2015). Conjunctive Coding of Complex Object Features. *Cerebral Cortex*, *26*(5), 2271–2282. https://doi.org/10.1093/cercor/bhv081

Esteban, O., Markiewicz, C. J., Blair, R. W., Moodie, C. A., Isik, A. I., Erramuzpe, A., … Gorgolewski, K. J. (2019). fMRIPrep: a robust preprocessing pipeline for functional MRI. *Nature Methods*, *16*(1), 111–116. https://doi.org/10.1038/s41592-018-0235-4

Esteban, O., Markiewicz, C. J., DuPre, E., Goncalves, M., Kent, J. D., Ciric, R., … Gorgolewski, K. J. (2018). FMRIPrep. *Software*, Zenodo. https://doi.org/https://doi.org/10.5281/zenodo.852659.

Fonov, V. S., Evans, A. C., McKinstry, R. C., Almli, C. R., & Collins, D. L. (2009). Unbiased nonlinear average age-appropriate brain templates from birth to adulthood. *NeuroImage*, *47*, Supplement 1: S102. https://doi.org/https://doi.org/10.1016/S1053-8119(09)70884-5

Glasser, M. F., Sotiropoulos, S. N., Wilson, J. A., Coalson, T. S., Fischl, B., Andersson, J. L., … Jenkinson, M. (2013). The minimal preprocessing pipelines for the Human Connectome Project. *NeuroImage*, *80*, 105–124. https://doi.org/10.1016/j.neuroimage.2013.04.127

Gorgolewski, K., Burns, C. D., Madison, C., Clark, D., Halchenko, Y. O., Waskom, M. L., & Ghosh, S. S. (2011). Nipype: A Flexible, Lightweight and Extensible Neuroimaging Data Processing Framework in Python. *Frontiers in Neuroinformatics*, *5*(13), 1–10. https://doi.org/10.3389/fninf.2011.00013

Greve, D. N., & Fischl, B. (2009). Accurate and robust brain image alignment using boundary-based registration. *NeuroImage*, *48*(1), 63–72. https://doi.org/10.1016/j.neuroimage.2009.06.060

Grill-Spector, K. (2003). The neural basis of object perception. *Current Opinion in Neurobiology*, *13*(2), 159–166. https://doi.org/10.1016/S0959-4388(03)00040-0

Grill-Spector, K., Kourtzi, Z., & Kanwisher, N. (2001). The lateral occipital complex and its role in object recognition. *Vision Research*, *41*(10–11), 1409–1422. https://doi.org/10.1016/S0042-6989(01)00073-6

Grill-Spector, K., Kushnir, T., Edelman, S., Avidan, G., Itzchak, Y., & Malach, R. (1999). Differential processing of objects under various viewing conditions in the human lateral occipital complex. *Neuron*. https://doi.org/10.1016/S0896-6273(00)80832-6

Gross, C. G., Cowey, A., & Manning, F. J. (1971). Further analysis of visual discrimination deficits following foveal prestriate and inferotemporal lesions in rhesus monkeys. *Journal of Comparative & Physiological Psychology*, *76*(1), 1–7.

Hadjikhani, N., Liu, A. K., Dale, A. M., Cavanagh, P., & Tootell, R. B. H. (1998). Retinotopy and color sensitivity in human visual cortical area V8. *Nature Neuroscience*, *1*(3), 235–241.

Hannula, D. E., Libby, L. A., Yonelinas, A. P., & Ranganath, C. (2013). Medial temporal

lobe contributions to cued retrieval of items and contexts. *Neuropsychologia*, *51*(12), 2322–2332. https://doi.org/10.1016/j.neuropsychologia.2013.02.011

Hassabis, D., Kumaran, D., Vann, S. D., & Maguire, E. A. (2007). Patients with hippocampal amnesia cannot imagine new experiences. *Proceedings of the National Academy of Sciences*, *104*(5), 1726–1731. https://doi.org/10.1073/pnas.0610561104

Hubel, D. H., & Wiesel, T. N. (1962). Receptive Fields, Binocular Interaction and Functional Architecture in the Cat's Visual Cortex. *Journal of Physiology*, *160*, 106–154.

Hubel, D. H., & Wiesel, T. N. (1965). Receptive Architecture in Two Nonstriate Visual Areas (18 and 19) of the Cat. *Journal of Neurophysiology*, *28*, 229–289.

Inhoff, M. C., Heusser, A. C., Tambini, A., Martin, C. B., O'Neil, E. B., Köhler, S., … Davachi, L. (2019). Understanding perirhinal contributions to perception and memory: Evidence through the lens of selective perirhinal damage. *Neuropsychologia*, *124*, 9–18. https://doi.org/10.1016/j.neuropsychologia.2018.12.020

Iwai, E., & Mishkin, M. (1968). Two visual foci in the temporal lobe of monkeys. In N. Yoshii & N. Buchwald (Eds.), *Neurophysiological basis of learning and behavior* (pp. 1–11). Japan: Osaka University Press.

Jenkinson, M., Bannister, P., Brady, M., & Smith, S. (2002). Improved Optimization for the Robust and Accurate Linear Registration and Motion Correction of Brain Images. *NeuroImage*, *17*(2), 825–841. https://doi.org/10.1006/nimg.2002.1132

Kanwisher, N. (2006). What's in a Face ? *Science*, *311*(February), 617–618.

Kanwisher, N., McDermott, J., & Chun, M. M. (1997). The fusiform face area: A module in human extrastriate cortex specialized for face perception. *The Journal of Neuroscience*, *17*(11), 4302–4311. https://doi.org/10.1098/Rstb.2006.1934

Karanian, J. M., & Slotnick, S. D. (2015). Memory for shape reactivates the lateral occipital complex. *Brain Research*, *1603*, 124–132. https://doi.org/10.1016/j.brainres.2015.01.024

Karanian, J. M., & Slotnick, S. D. (2017). False memories for shape activate the lateral occipital complex. *Learning & Memory*, *24*(10), 552–556. https://doi.org/10.1101/lm.045765.117.24

Karanian, J. M., & Slotnick, S. D. (2018). Confident false memories for spatial location are mediated by V1. *Cognitive Neuroscience*, *9*(3–4), 139–150. https://doi.org/10.1080/17588928.2018.1488244

Kent, B. A., Hvoslef-Eide, M., Saksida, L. M., & Bussey, T. J. (2016). The representational–hierarchical view of pattern separation: Not just hippocampus, not

just space, not just memory? *Neurobiology of Learning and Memory*, *129*, 99–106. https://doi.org/10.1016/j.nlm.2016.01.006

Kim, H. (2010). Dissociating the roles of the default-mode, dorsal, and ventral networks in episodic memory retrieval. *NeuroImage*, *50*, 1648–1657. https://doi.org/10.1016/j.neuroimage.2010.01.051

Kim, S., Dede, A. J. O., Hopkins, R. O., & Squire, L. R. (2015). Memory, scene construction, and the human hippocampus. *Proceedings of the National Academy of Sciences*, *112*(15), 4767–4772. https://doi.org/10.1073/pnas.1503863112

Kim, T., Bair, W., & Pasupathy, A. (2019). Neural Coding for Shape and Texture in Macaque Area V4. *The Journal of Neuroscience*, *39*(24), 4760–4774.

Klein, A., Ghosh, S. S., Bao, F. S., Giard, J., Häme, Y., Stavsky, E., … Keshavan, A. (2017). Mindboggling morphometry of human brains. *PLOS Computational Biology*, *13*(2), e1005350. https://doi.org/10.1371/journal.pcbi.1005350

Kobatake, E., & Tanaka, K. (1994). Neuronal selectivities to complex object features in the ventral visual pathway of the macaque cerebral cortex. *Journal of Neurophysiology*, *71*(3), 856–867. https://doi.org/10.1038/476265a

Kriegeskorte, N., Goebel, R., & Bandettini, P. (2006). Information-based functional brain mapping. *Proceedings of the National Academy of Sciences*, *103*(10), 3863–3868. https://doi.org/10.1073/pnas.0600244103

Kriegeskorte, Nikolaus, Simmons, W. K., Bellgowan, P. S. F., & Baker, C. I. (2009). Circular analysis in systems neuroscience: the dangers of double dipping. *Nature Neuroscience*, *12*(5), 535–540. https://doi.org/10.1167/8.6.88

Lacot, E., Vautier, S., Kőhler, S., Pariente, J., Martin, C. B., Puel, M., … Barbeau, E. J. (2017). Familiarity and recollection vs representational models of medial temporal lobe structures: A single-case study. *Neuropsychologia*, *104*(July), 76–91. https://doi.org/10.1016/j.neuropsychologia.2017.07.032

Lanczos, C. (1964). Evaluation of Noisy Data. *Journal of the Society for Industrial and Applied Mathematics Series B Numerical Analysis*, *1*(1), 76–85.

Lashley, K. S. (1950). In search of the engram. In *Society of Experimental Biology Symposium No. 4: Physiological mechanisms in animal behaviour* (pp. 454–482). Cambridge, England: Cambridge University Press.

Lee, A. C. H. (2006). Differentiating the Roles of the Hippocampus and Perirhinal Cortex in Processes beyond Long-Term Declarative Memory: A Double Dissociation in Dementia. *Journal of Neuroscience*, *26*(19), 5198–5203. https://doi.org/10.1523/JNEUROSCI.3157-05.2006

Lee, A. C. H., Barense, M. D., & Graham, K. S. (2005). The contribution of the human

medial temporal lobe to perception: bridging the gap between animal and human studies. *The Quarterly Journal of Experimental Psychology*, *58*(3–4), 300–325. https://doi.org/10.1080/02724990444000168

Lee, A. C. H., Buckley, M. J., Pegman, S. J., Spiers, H., Scahill, V. L., Gaffan, D., … Graham, K. S. (2005). Specialization in the medial temporal lobe for processing of objects and scenes. *Hippocampus*, *15*, 782–797. https://doi.org/10.1002/hipo.20101

Lee, A. C. H., Bussey, T. J., Murray, E. A., Saksida, L. M., Epstein, R. A., Kapur, N., … Graham, K. S. (2005). Perceptual deficits in amnesia: Challenging the medial temporal lobe "mnemonic" view. *Neuropsychologia*, *43*(1), 1–11. https://doi.org/10.1016/j.neuropsychologia.2004.07.017

Lee, A. C. H., Yeung, L.-K., & Barense, M. D. (2012). The hippocampus and visual perception. *Frontiers in Human Neuroscience*, *6*(April), 91. https://doi.org/10.3389/fnhum.2012.00091

Lee, S.-H., Kravitz, D. J., & Baker, C. I. (2019). Differential Representations of Perceived and Retrieved Visual Information in Hippocampus and Cortex. *Cerebral Cortex*, *29*(10), 4452–4461. https://doi.org/10.1093/cercor/bhy325

Maguire, E. a., Intraub, H., & Mullally, S. L. (2015). Scenes, Spaces, and Memory Traces: What Does the Hippocampus Do? *The Neuroscientist*, 1073858415600389. https://doi.org/10.1177/1073858415600389

Malach, R., Reppas, J., Benson, R., Kwong, K., Jiang, H., Kennedy, W., … Tootell, R. (1995). Object-related activity revealed by functional magnetic resonance imaging in human occipital cortex. *Proceedings of the National Academy of Sciences of the United States of America*, *92*(August), 8135–8139.

Mandler, G. (1980). Recognizing: The judgment of previous occurrence. *Psychological Review*, *87*(3), 252–271. https://doi.org/10.1037/0033-295X.87.3.252

Martin, C. B., Douglas, D., Newsome, R. N., Man, L. L. Y., & Barense, M. D. (2018). Integrative and distinctive coding of visual and conceptual object features in the ventral visual stream. *ELife*, *7*, 1–29. https://doi.org/10.7554/elife.31873

Mazer, J. A., Vinje, W. E., McDermott, J., Schiller, P. H., & Gallant, J. L. (2002). Spatial frequency and orientation tuning dynamics in area V1. *Proceedings of the National Academy of Sciences*, *99*(3), 1645–1650. https://doi.org/10.1073/pnas.022638499

McTighe, S. M., Cowell, R. A., Winters, B. D., Bussey, T. J., & Saksida, L. M. (2010). Paradoxical false memory for objects after brain damage. *Science*, *330*, 1408–1410. https://doi.org/10.1126/science.1194780

Meunier, M., Bachevalier, J., Mishkin, M., & Murray, E. a. (1993). Effects on visual recognition of combined and separate ablations of the entorhinal and perirhinal cortex in rhesus monkeys. *The Journal of Neuroscience : The Official Journal of the*

Society for Neuroscience, *13*(12), 5418–5432.

Mullally, S. L., & Maguire, E. A. (2013). Memory, Imagination, and Predicting the Future: A Common Brain Mechanism? *The Neuroscientist : A Review Journal Bringing Neurobiology, Neurology and Psychiatry*, *20*(3), 220–234. https://doi.org/10.1177/1073858413495091

Mumford, J. A., Turner, B. O., Ashby, F. G., & Poldrack, R. A. (2012). Deconvolving BOLD activation in event-related designs for multivoxel pattern classification analyses. *NeuroImage*, *59*(3), 2636–2643. https://doi.org/10.1016/j.neuroimage.2011.08.076

Norman, K. A., & O'Reilly, R. C. (2003). Modeling hippocampal and neocortical contributions to recognition memory: A complementary-learning-systems approach. *Psychological Review*, *110*(4), 611–646. https://doi.org/10.1037/0033-295X.110.4.611

O'Keefe, J., & Dostrovsky, J. (1971). The hippocampus as a spatial map: Preliminary evidence from unit activity in the freely-moving rat. *Brain Research*, *34*(1), 171–175. Retrieved from http://www.ncbi.nlm.nih.gov/pubmed/5124915

O'Keefe, J., & Nadel, L. (1978). *The hippocampus as a cognitive map*. Oxford University Press.

Olman, C. A., Davachi, L., & Inati, S. (2009). Distortion and signal loss in medial temporal lobe. *PLoS ONE*, *4*(12). https://doi.org/10.1371/journal.pone.0008160

Oosterhof, N. N., Connolly, A. C., & Haxby, J. V. (2016). CoSMoMVPA: Multi-Modal Multivariate Pattern Analysis of Neuroimaging Data in Matlab/GNU Octave. *Frontiers in Neuroinformatics*, *10*(July), 1–27. https://doi.org/10.3389/fninf.2016.00027

Palombo, D. J., Hayes, S. M., Peterson, K. M., Keane, M. M., & Verfaellie, M. (2016). Medial Temporal Lobe Contributions to Episodic Future Thinking: Scene Construction or Future Projection? *Cerebral Cortex*, 1–12. https://doi.org/10.1093/gbe/evw245

Petersen, R. C., Parisi, J. E., Dickson, D. W., Johnson, K. A., Knopman, D. S., Boeve, B. F., … Kokmen, E. (2006). Neuropathologic features of amnestic mild cognitive impairment. *Archives of Neurology*, *63*, 665–672.

Power, J. D., Mitra, A., Laumann, T. O., Snyder, A. Z., Schlaggar, B. L., & Petersen, S. E. (2014). Methods to detect, characterize, and remove motion artifact in resting state fMRI. *NeuroImage*, *84*, 320–341. https://doi.org/10.1016/j.neuroimage.2013.08.048

Ranganath, C., & Ritchey, M. (2012). Two cortical systems for memory-guided behaviour. *Nature Reviews Neuroscience*, *13*(10), 713–726.

https://doi.org/10.1038/nrn3338

Restivo, L., Vetere, G., Bontempi, B., & Ammassari-teule, M. (2009). The Formation of Recent and Remote Memory Is Associated with Time-Dependent Formation of Dendritic Spines in the Hippocampus and Anterior Cingulate Cortex. *Journal of Neuroscience*, *29*(25), 8206–8214. https://doi.org/10.1523/JNEUROSCI.0966-09.2009

Reuter, M., Rosas, H. D., & Fischl, B. (2010). Highly accurate inverse consistent registration: A robust approach. *NeuroImage*, *53*(4), 1181–1196. https://doi.org/10.1016/j.neuroimage.2010.07.020

Riesenhuber, M., & Poggio, T. (1999). Hierarchical models of object recognition in cortex. *Nature Neuroscience*, *2*(11), 1019–1025. https://doi.org/10.1038/14819

Ritchey, M., Montchal, M. E., Yonelinas, A. P., & Ranganath, C. (2015). Delay-dependent contributions of medial temporal lobe regions to episodic memory retrieval. *ELife*, *4*, 1–19. https://doi.org/10.7554/eLife.05025

Robin, J., Rai, Y., Valli, M., & Olsen, R. (2019). Category specificity in the medial temporal lobe: A systematic review. *Hippocampus*, *29*, 313–339. https://doi.org/10.1002/hipo.23024

Rosenbaum, R. S., Gilboa, A., & Moscovitch, M. (2014). Case studies continue to illuminate the cognitive neuroscience of memory. *Annals of the New York Academy of Sciences*, *1316*(1), 105–133. https://doi.org/10.1111/nyas.12467

Ross, D. A., Sadil, P., Wilson, D. M., & Cowell, R. A. (2018). Hippocampal engagement during recall depends on memory content. *Cerebral Cortex, 28*(8). https://doi.org/10.1093/cercor/bhx147

Rugg, M. D., & Vilberg, K. L. (2013). Brain networks underlying episodic memory retrieval. *Current Opinion in Neurobiology*, *23*(2), 255–260. https://doi.org/10.1016/j.conb.2012.11.005

Rust, N. C., & DiCarlo, J. J. (2012). Balanced Increases in Selectivity and Tolerance Produce Constant Sparseness along the Ventral Visual Stream. *Journal of Neuroscience*, *32*(30), 10170–10182. https://doi.org/10.1523/jneurosci.6125-11.2012

Saksida, L. M., Bussey, T. J., Buckmaster, C. A., & Murray, E. A. (2006). No effect of hippocampal lesions on perirhinal cortex-dependent feature-ambiguous visual discriminations. *Hippocampus*, *16*(4), 421–430. https://doi.org/10.1002/hipo.20170

Satterthwaite, T. D., Elliott, M. A., Gerraty, R. T., Ruparel, K., Loughead, J., Calkins, M. E., … Wolf, D. H. (2013). An improved framework for confound regression and filtering for control of motion artifact in the preprocessing of resting-state functional connectivity data. *NeuroImage*, *64*(1), 240–256.

https://doi.org/10.1016/j.neuroimage.2012.08.052

Scoville, W. B., & Milner, B. (1957). Loss of recent memory after bilateral hippocampal lesions. *The Journal of Neuropsychiatry and Clinical Neurosciences*, *20*(11), 11–21. https://doi.org/10.1136/jnnp.20.1.11

Shimamura, A. P. (2011). Episodic retrieval and the cortical binding of relational activity. *Cognitive, Affective, & Behavioral Neuroscience*, *11*, 277–291. https://doi.org/10.3758/s13415-011-0031-4

Slotnick, S. D. (2009). Memory for color reactivates color processing region. *NeuroReport*, *20*(17), 1568–1571. https://doi.org/10.1097/WNR.0b013e328332d35e

Smith, S. M., Jenkinson, M., Woolrich, M. W., Beckmann, C. F., Behrens, T. E. J., Johansen-berg, H., … Matthews, P. M. (2004). Advances in functional and structural MR image analysis and implementation as FSL. *Neuroimage*, *23*(Suppl. 1), S208-219. https://doi.org/10.1016/j.neuroimage.2004.07.051

Squire, L. R. (2009). The legacy of patient H.M. for neuroscience. *Neuron*, *61*(1), 6–9. https://doi.org/10.1016/j.neuron.2008.12.023

Squire, L. R., & Zola-Morgan, S. (1991). The medial temporal lobe memory system. *Science*, *253*, 1380–1386. https://doi.org/10.1126/science.1896849

Staresina, B. P., Cooper, E., & Henson, R. N. (2013). Reversible Information Flow across the Medial Temporal Lobe: The Hippocampus Links Cortical Modules during Memory Retrieval. *Journal of Neuroscience*, *33*(35), 14184–14192. https://doi.org/10.1523/JNEUROSCI.1987-13.2013

Suzuki, W. A. (2010). Untangling memory from perception in the medial temporal lobe. *Trends in Cognitive Sciences*, *14*(5), 195–200. https://doi.org/10.1016/j.tics.2010.02.002

Thakral, P. P., Slotnick, S. D., & Schacter, D. L. (2013). Conscious processing during retrieval can occur in early andlate visual regions. *Neuropsychologia*, *51*(3), 482–487. https://doi.org/10.1016/j.neuropsychologia.2012.11.020.Conscious

Thakral, P. P., Wang, T. H., & Rugg, M. D. (2017). Decoding the content of recollection within the core recollection network and beyond. *Cortex*, *91*, 101–113. https://doi.org/10.1016/j.cortex.2016.12.011.Decoding

Tustison, N. J., Avants, B. B., Cook, P. A., Yuanjie Zheng, Egan, A., Yushkevich, P. A., & Gee, J. C. (2010). N4ITK: Improved N3 Bias Correction. *IEEE Transactions on Medical Imaging*, *29*(6), 1310–1320. https://doi.org/10.1109/TMI.2010.2046908

Tyler, L. K., Chiu, S., Zhuang, J., Randall, B., Devereux, B. J., Wright, P., … Taylor, K. I. (2013). Objects and categories: Feature statistics and object processing in the ventral stream. *Journal of Cognitive Neuroscience*, *25*(10), 1723–1735.

https://doi.org/10.1162/jocn

Ungerleider, L. G., & Mishkin, M. (1982). Two cortical visual systems. In D. G. Ingle, M. A. Goodale, & R. J. W. Mansfield (Eds.), *Analysis of Visual Behavior* (pp. 549–586). Cambridge, MA: MIT Press. https://doi.org/10.2139/ssrn.1353746

van den Honert, R. N., McCarthy, G., & Johnson, M. K. (2017). Holistic versus feature-based binding in the medial temporal lobe. *Cortex*, *91*, 56–66. https://doi.org/10.1016/j.cortex.2017.01.011

Wang, L., Mruczek, R. E. B., Arcaro, M. J., & Kastner, S. (2015). Probabilistic maps of visual topography in human cortex. *Cerebral Cortex*, *25*(10), 3911–3931. https://doi.org/10.1093/cercor/bhu277

Williams, P. (1998). Representational organization of multiple examplars of object categories, 1–21.

Wilson, M., Kaufman, H. M., Zieler, R. E., & Lieb, J. P. (1972). Visual identification and memory in monkeys with circumscribed inferotemporal lesions. *Journal of Comparative and Physiological Psychology*, *78*(2), 173–183.

Winters, B. D., Forwood, Suzanna, E., Cowell, Rosemary, A., Saksida, Lisa, M., & Bussey, T. J. (2004). Double dissociation between the effects of peri-postrhinal cortex and hippocampal lesions on tests of object recognition and spatial memory: Heterogeneity of function within the temporal lobe. *Journal of Neuroscience*, *24*(26), 5901–5908. https://doi.org/10.1523/JNEUROSCI.1346-04.2004

Yau, J. M., Pasupathy, A., Brincat, S. L., & Connor, C. E. (2013). Curvature Processing Dynamics in Macaque Area V4. *Cerebral Cortex*, *23*(1), 198–209. https://doi.org/10.1093/cercor/bhs004

Yeung, L.-K., Ryan, J. D., Cowell, R. A., & Barense, M. D. (2013). Recognition memory impairments caused by false recognition of novel objects. *Journal of Experimental Psychology: General*, *142*(4), 1384–1397. https://doi.org/10.1037/a0034021

Yonelinas, A. P., Aly, M., Wang, W., & Koen, J. D. (2010). Recollection and familiarity: Examining controversial assumptions and new directions. *Hippocampus*, *20*(11), 1178–1194. https://doi.org/10.1002/hipo.20864

Zeidman, P., Mullally, S. L., & Maguire, E. A. (2015). Constructing, perceiving, and maintaining scenes: Hippocampal activity and connectivity. *Cerebral Cortex*, *25*(10), 3836–3855. https://doi.org/10.1093/cercor/bhu266

Zhang, Y., Brady, M., & Smith, S. (2001). Segmentation of brain MR images through a hidden Markov random field model and the expectation-maximization algorithm. *IEEE Transactions on Medical Imaging*, *20*(1), 45–57. https://doi.org/10.1109/42.906424